University of BRISTOL

AVDASI 4 – AENGM0060

FW1 – Final Engineering Design Report

Advisor: Mark Lowenberg

December 2020

Nicolas Barra	nb17010	Chief Engineer; Aerodynamics
Joaquim Bolos	jb17029	Aircraft Structure, CAD and Systems Integration
Will Gale	wg17230	Project Manager; Economics and Business Case
William Haigh	wh17435	Operational Performance and Propulsion
Charlie Mourant	cm17855	Weight, Balance, Stability and Flight Control
Mamunur Rashid	mr17263	Alternative Technologies Impacting Noise and Emissions
Tsz Pok Lam	tl17144	Structures and Manufacturing
Yiling Zheng	yz17853	Landing Gear and Fuel Systems

Abstract

This report outlines FW1's final design for a 120 pax aircraft and a concept for a zero-emission variant. The aim of the project was to produce a fuel burn-optimised kerosene-burning turbofan aircraft, alongside a second variant with no carbon emissions. A concept down selection process was followed to identify the most promising initial configuration, which was a conventional, high AR, low sweep aircraft, and then an iterative process was followed to refine that concept into a final design that burns 29% less fuel than an A220-100 over a 500nmi mission. The design was optimised by focusing on mitigating induced drag and sizing the engine to maximise fuel efficiency. An investigation into available zero carbon emission technologies found that liquid hydrogen combustion propulsion would provide the fastest time to market and require the fewest modifications to the baseline design. The zero-emission variant employs front and rear cryogenic liquid hydrogen tanks in an extended fuselage and modified gas turbine engines.

Contents

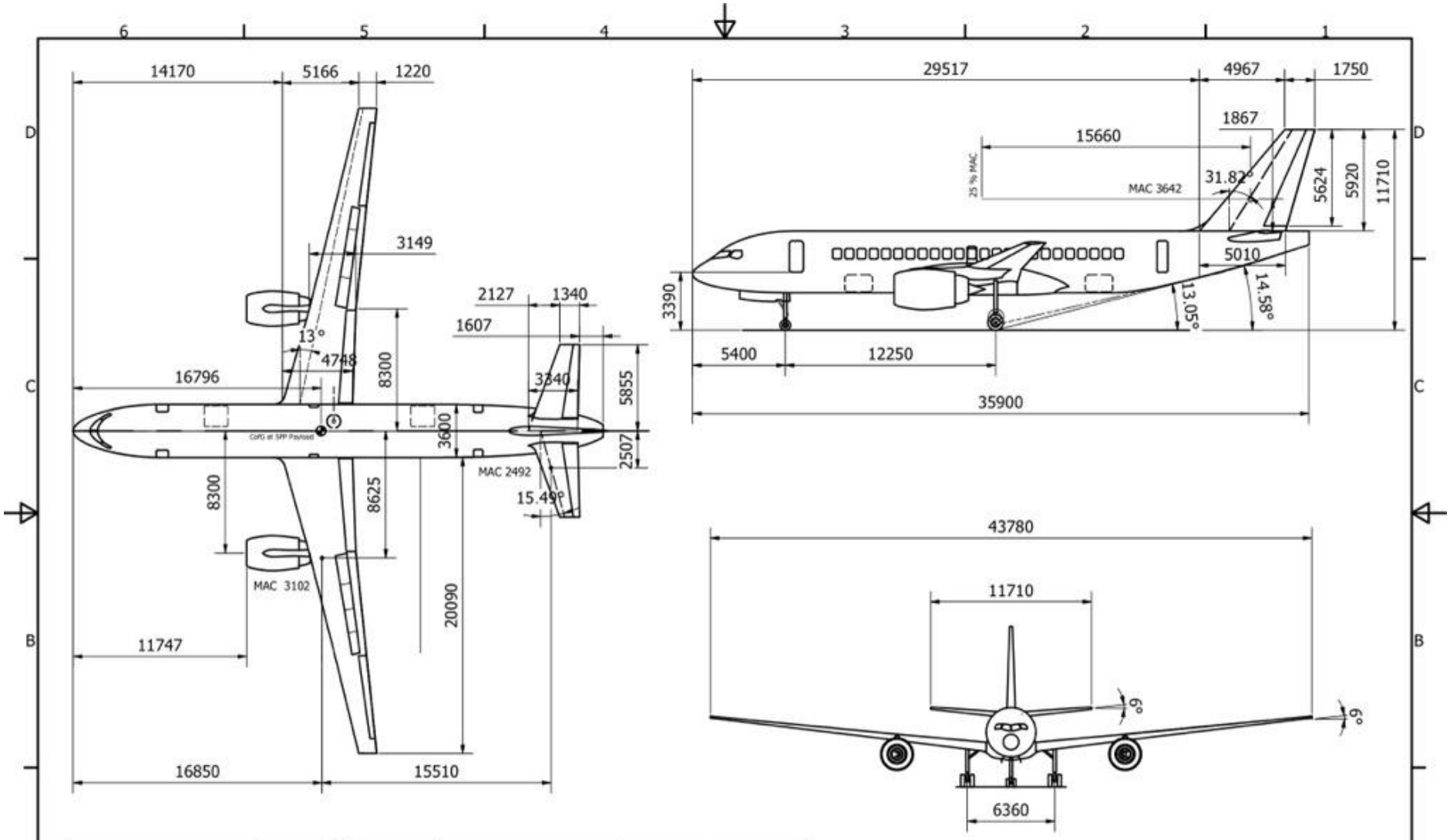

	Wing	HTP	VTP
Ref Area	109.62	27.405	20
AR	18	5	1.8
1/4 Chord Sweep	13	15.45	31.82
Taper Ratio	0.66/0.38	0.4	0.5
T/C Ratio	14/14/10	12	12

DESIGNED BY	CHECKED BY	APPROVED BY	DATE	Units	DATE	
Joaquim Bolós	Charles Mouran	Nick Barra	09/12/2020	mm	06/12/2020	A4

University of BRISTOL

FW1 General Arrangement

BSI | ISSUE 1 | SHEET 1 / 1

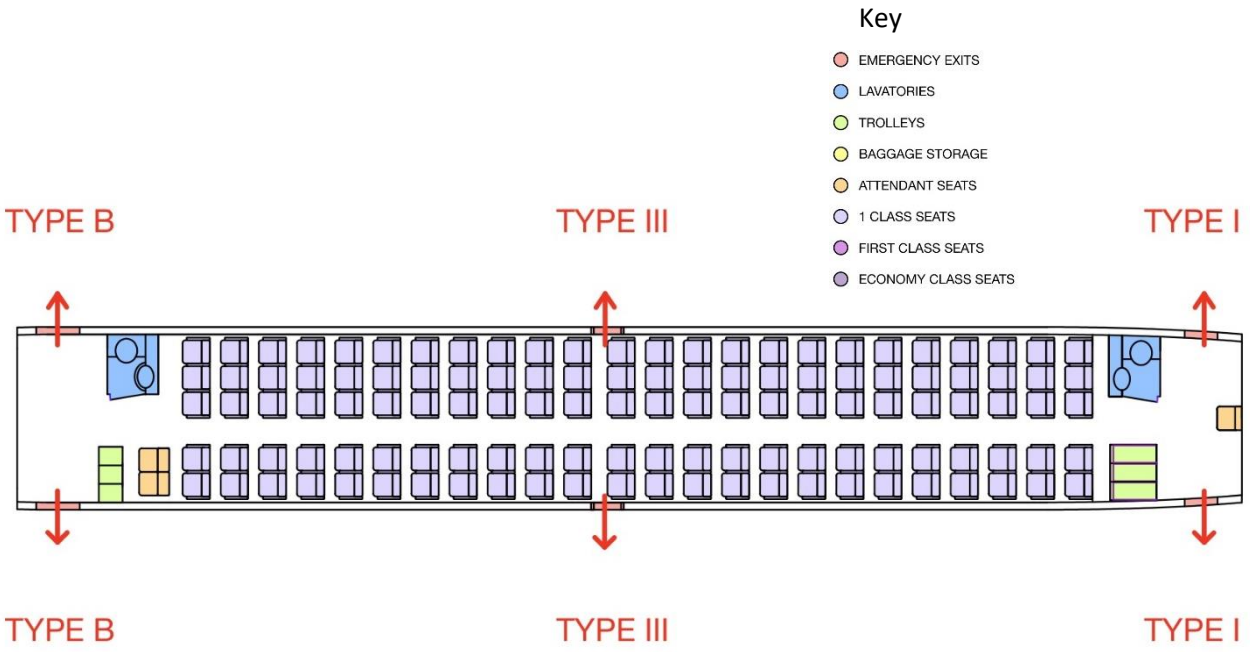

Figure 1: High-density cabin layout; 120pax

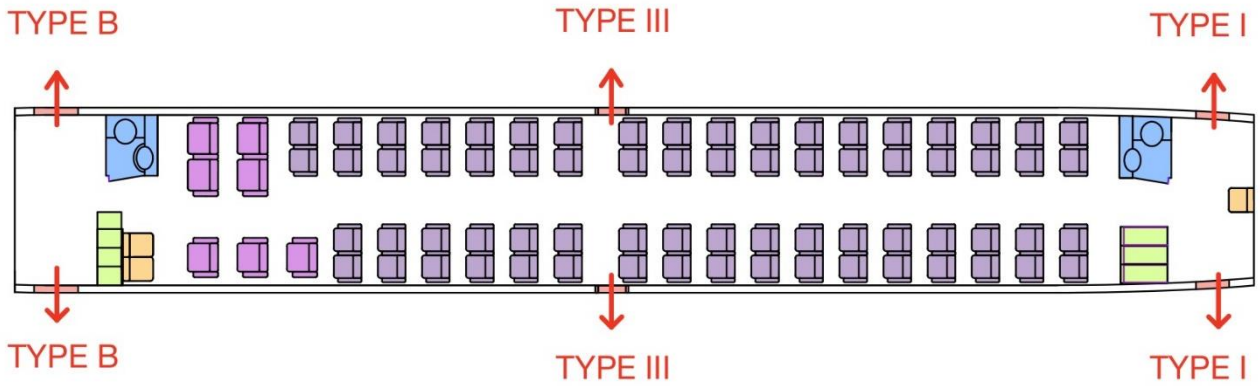

Figure 2: Two-class cabin layout; 79 pax

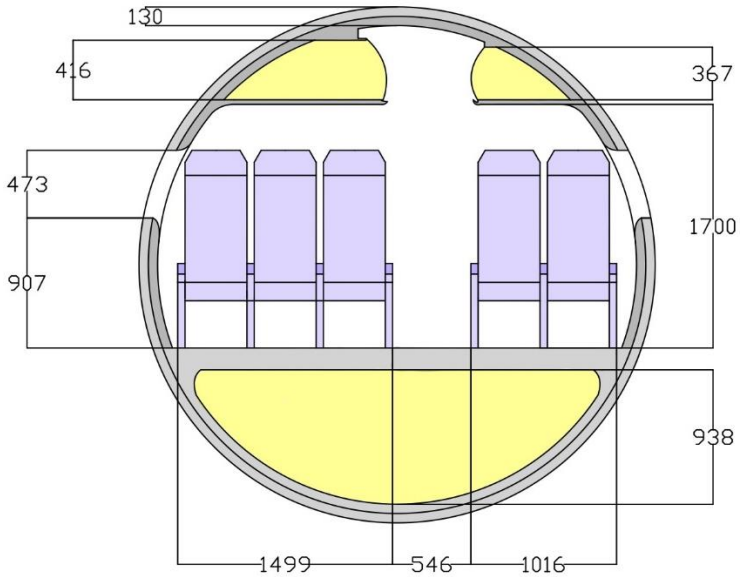

Figure 3: High-density cabin cross-section, dimensions in mm

Data Sheet

Item	Value	Units	Additional Comments
Configuration			Conventional, Low Sweep, High AR, Turbofan
Maximum Take-Off Weight	42,480	kg	
Operators Weight Empty	25,243	kg	
Fuel for design mission 1000 nm	3,073	kg	
Fuel for 500 nm	1,776	kg	
Payload for design mission	12,600	kg	
Maximum Landing Weight	40,476	kg	
Maximum Zero Fuel Weight	38,741	kg	
Maximum Fuel Capacity	4,652	kg	
Cruise Mach No	0.67M		
VCr/MCr (VCr in kts CAS)	224	kts CAS	
Initial Cruise Altitude	35,000	ft	
L/D (start of Cruise)	23.2		
Take-Off Field Length	1,870	m	
Landing Field Length	1,560	m	
Approach Speed	125	kts	
Fuselage Length	35.9	m	
Fuselage Width (or Diameter if circular)	3.6	m	
Fuselage Height or Depth	3.6	m	
Wing Area	109.6	m^2	
Span	43.78	m	
Aspect Ratio	18		
Thickness of Wing @ outer wing (t/c)	0.12		
Taper Ratio	0.3		
Mean Aerodynamic Chord	3.10	m	
Sweep @ 1/4 Chord	13	degs	
High Lift System (trailing edge)	Plain Flap		
High Lift System (leading edge)	None		
CLmax	2.4		
Distance of wing LE at root from nose	14.17	m	
Distance of wing MAC from datum	9.01	m	spanwise from fuselage centre line
Tailplane Area	27.41	m^2	
Span	11.71	m	
Aspect Ratio	5		
1/4 Chord MAC (wing) to 1/4 Chord MAC (tailplane)	15.51	m	
Fin Area	20	m^2	
Span	6.4	m	
Aspect Ratio	1.8		
1/4 Chord MAC (wing) to 1/4 Chord MAC (fin)	15.66	m	
Number of Engines	2		
Engine position (wing/fuselage/other)	Wing		
Engine Type	Turbofan		
Sea Level Static Thrust (per Engine)	14,163	lb	
Thrust at Initial Cruise Altitude (per Engine)	2,335	lb	
Engine Thrust Scale Factor	0.94		
Engine Fan or Propeller Diameter	1.9	m	
SFC at mid cruise (500nmi study mission)	0.5286	lbm/hr/lbf	
Landing Gear Layout	Tricycle		
Main Landing Gear Tyre Size	36x11.0R18	inches	
Main Landing Gear Geometry for ACN	400	mm	
ACN	21		(flexible pavement subgrade B)
Height of Fuselage Datum above Ground	3.52	m	
CG range at MTOW	29	% MAC	
Aircraft NRC	3,729	Million $	
Aircraft RC	37	Million $	
Manufacture's Study Price	60	Million $	
Engine Price (per engine)	6	Million $	
Aircraft DOC	11,064	$/trip	500nmi trip with std pax P/L
Turnaround time	30	mins	
Refuel time	6	mins	
Trim Tank yes/no	No		

Nomenclature

AASI	Aircraft Architecture & Systems Integration
ACN	Aircraft Classification Number
APU	Auxiliary Power Unit
AR	Aspect Ratio
ATNE	Alternative Technologies for Noise and emissions
BLI	Boundary Layer Ingestion
BPR	Bypass Ratio
BSI	British Standards Institution
BWB	Blended Wing Body
CAD	Computer Aided Design
CAS	Calibrated Airspeed
CFD	Computational Fluid Dynamics
CFRP	Carbon Fibre Reinforced Polymer
CG	Centre of Gravity
C_L	Lift Coefficient
C_{Lmax}	Maximum Lift Coefficient
CM	Configuration Management
CML	Continuous Mold-line Link
COC	Cash Operating Costs
DOC	Direct Operating Costs
EGTS	Electric Green Taxiing System
EIS	Entry into Service
FAR	Federal Aviation Regulations
FDR	Final Design Review
FEA	Finite Element Analysis
GHG	Greenhouse Gas
GLARE	Glass Laminate Aluminium Reinforced Epoxy
HTP	Horizontal Tailplane
ICA	Initial Cruise Altitude
ICAO	International Civil Aviation Organisation
ISA	International Standard Atmosphere
L/D	Lift-to-Drag Ratio
LE	Leading Edge
LFC	Laminar Flow Control
LH_2	Liquid Hydrogen
MAC	Mean Aerodynamic Chord
MLG	Main Landing Gear
MLW	Maximum Landing Weight
MSP	Manufacturer's Study Price
MTOW	Maximum Take-Off Weight
NLG	Nose Landing Gear
NO_x	Nitrous Oxides
NRC	Non-Recurring Costs
OEI	One Engine Inoperative
RC	Recurring Costs
SAR	Specific Air Range
SFC	Specific Fuel Consumption
SPP	Standard Passenger Payload
t/c	Thickness-to-Chord Ratio
TE	Trailing Edge
TRL	Technology Readiness Level
VTP	Vertical Tailplane
EHA	Electro-Hydraulic Actuator
EMA	Electro-Mechanical Actuator

1 Introduction

With climate change becoming an increasingly important consideration for global policy and business, it is imperative to attempt to tackle the problem from all angles, including the design of future aircraft. Not only does the aerospace industry contribute toward greenhouse gas emissions, but those emitted by aircraft are mostly done so directly into the atmosphere. As such, Airbus require a design for a short-range, fuel burn-optimised airliner.

While attempting to minimise both the noise and fuel emissions, the aircraft design must achieve several things: support for 120 passengers in a high-density configuration, a design range of 1,000nmi, turbofan propulsion, all technology needs to be ready for first flight by 2027 and compatibility with ICAO code D gates (52m max. wingspan) is required.

To best understand the gap in the market that needs filling, the market and requirements were analysed and evaluated, laying the groundwork for the generation and subsequent down selection of several design concepts to produce a finalised configuration that would best meet the requirements. After defining key aspects of the finalised concept, major challenges and risks that the design may face moving forward are discussed, a concept for a zero-emission variant is outlined and the aircraft is analysed economically. This is followed by a critical analysis of the design and the team's way of working. Finally, conclusions are drawn from the design and project.

2 Concept Selection and Justification

2.1 Market and Requirements Analysis

The first step in the design process was the determination of key design drivers and identification of the aircraft's position in the market. This process involved first researching existing aircraft of similar passenger capacities and ranges to identify competitors, ways in which the specification challenges conventional design approaches and key challenges that arise when designing short-haul passenger aircraft. Figure 4 shows how the aircraft compares to others in terms of its range and passenger capacity. Even though the surrounding market is relatively competitive, there is a definite lack of aircraft that fall in the high capacity, short-range region; the closest competitor is the Comac ARJ21-90, with a passenger capacity of 105pax and a range of 1100nmi. The lack of similar, fuel-burn optimised aircraft could mean that our aircraft's competitiveness is likely to be high, especially given the rising importance of environmental impact in the aerospace industry.

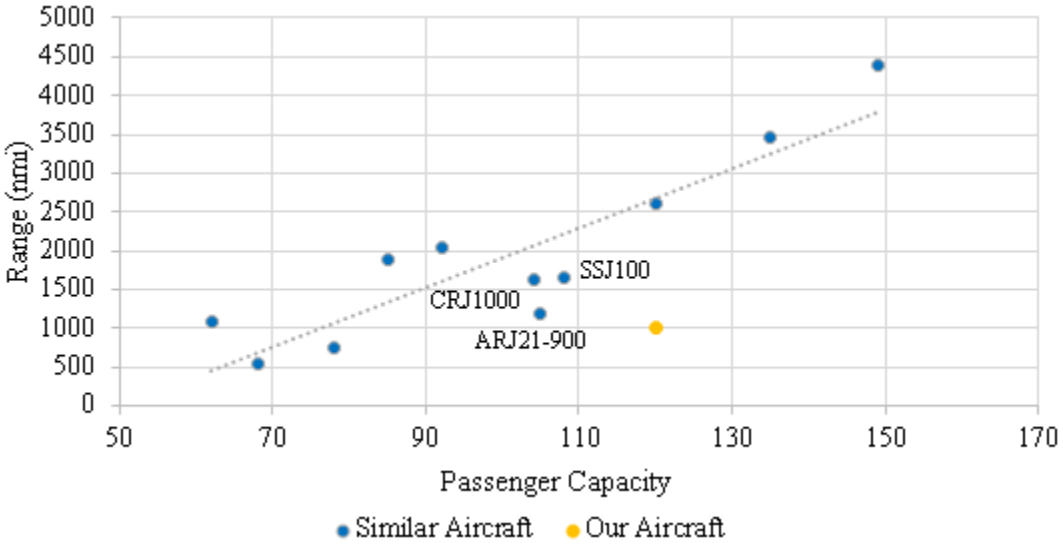

Figure 4: Illustration of competitor aircraft and the surrounding market

Market research established that the most common European journey in 2018 was on intra-European routes [1], with the LDN-FRA and LDN-DUB among the ten busiest European routes, indicating high demand for journeys less than 1000nmi. Therefore, an aircraft optimised for these ranges would likely be more competitive in terms of fuel burn than much of the existing fleet. A travel route investigation found that 500nmi journeys

from Bristol Airport reach most Alps-accessible airports. A range of 1,000nmi encompasses many popular summer holiday destinations, including the south of Spain and parts of Italy.
Airbus [2] predicts that the aerospace industry will continue growing at an annual rate of 4.3%, requiring almost 40,000 new passenger and freighter aircraft over the next two decades. Additionally, Airbus predicts that oil prices will rise over the next 20 years, potentially reaching $104 per barrel. With approximately 20% of a short-range aircraft's direct operating costs coming from fuel, this gives a financial incentive for airliners to consider fuel-burn optimised aircraft, alongside the moral consideration of climate change and possible legislature penalising emissions.

Successful fulfilment of the project requires an understanding of the requirement specification and the impacts that given requirements may have on concept generation, assessment and detailed design. Clarification of the importance and impacts of each requirement involved decomposition into hard and soft requirements. Hard requirements were selected based on their importance to the mission as these must be met, driving the initial sizing and concept design phases. Soft requirements, though deemed less critical to the success of the aircraft, were still endeavoured to be met. Also extracted were secondary key design drivers, after fuel burn minimisation, of direct operating costs, maintenance and airport compatibility.

2.2 Preliminary Concept Research

As there are many major conceptual possibilities to consider, the team divided into several smaller disciplines for a better breadth and depth of research. For each discipline, team members delivered a list of options and their impacts on the performance and design of a concept aircraft, in particular aerodynamic efficiency, weight and design viability, driven by the hard requirements in the requirement specification. The areas researched and options produced were:

- **Wing Planform –** Regular cantilever, blended wing body, delta wing, oblique wing
- **Wing Position –** Low, mid, high
- **Empennage –** Conventional, T-tail, cruciform, lifting canard, control canard, three lifting surface, V-tail, Y-tail, triple
- **Propulsion –** High BPR turbofan, low BPR turbofan, turboprop, wing-mounted, fuselage-mounted, buried
- **Landing Gear –** Tricycle, bicycle, tail dragger, quadricycle
- **Fuselage –** circular, elliptical, double bubble, varying geometry
- **Future Technologies –** hinged wingtips, electric green taxiing system (EGTS), boundary layer ingestion (BLI) engines, composite materials

2.3 Preliminary Concepts

The formulation of eight concepts followed the above research, exploring a range of possibilities and variations in the researched categories. Each design developed either from research into futuristic concepts or through consideration of the key design drivers and integration of different features. The concepts are laid out in Figure 5 and individually analysed below.

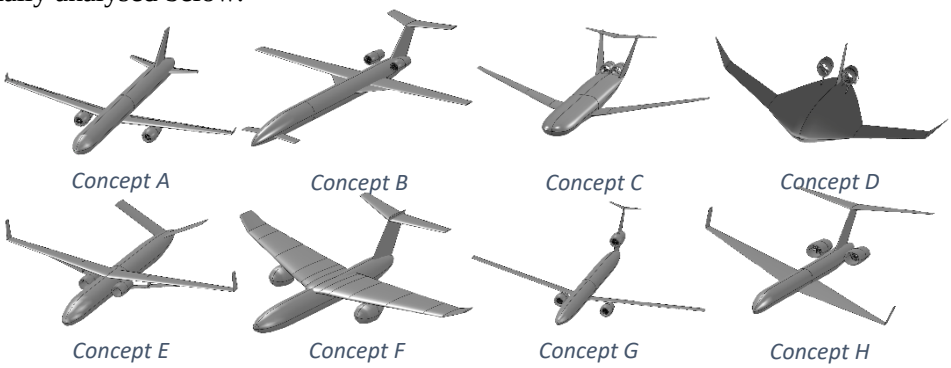

Figure 5: Initial design concepts

2.3.1 Concept A: High AR, Low Wing

Concept A was a low-wing aircraft with wing-mounted engines, a conventional tail and a four-abreast seating arrangement. The concept had a large aspect ratio and wingtip devices, reducing the induced drag of the aircraft. The wing-mounted engines would produce bending relief and would be easily accessible for

maintenance; however, they may also require longer, heavier landing gear for sufficient ground clearance. The conventional tail would be lighter than other options and provide simple, predictable control responses.

2.3.2 Concept B: Three Lifting Surface

The second concept utilised three lifting surfaces and a mid-mounted wing to try to limit weight and interference drag. The mid-mounted wing would produce less drag but also present stability and control issues due to its position behind the cabin. The three-lifting surface approach shifts some of the pitching moment onto the canard, reducing the downforce required by the tail and effectively reducing surface areas and weights of all three surfaces. The rear-mounted engines would have good OEI performance but would be harder to reach for maintenance and may negatively affect airflow over the wing and tail surfaces.

2.3.3 Concept C: Double Bubble

Concept C was an unconventional design connecting two adjacent fuselage sections to increase passenger capacity and allow the fuselage to contribute to the lift generation, reducing the required wing size. Rear-mounted BLI engines would help energise the fuselage's boundary layer to reduce drag, and the H-tail would be structurally efficient. However, the fuselage structure and control systems for such a short aircraft would be quite complex. Additionally, fuselage-mounted engines would produce a lot of cabin noise, and BLI engines are a novel concept that may not be ready by 2027.

2.3.4 Concept D: Blended-Wing-Body

Concept D was a BWB aircraft, with the fuselage and wing connecting very smoothly to form one large, aerodynamically efficient aircraft. The concept facilitated a very high lift to drag ratio and used BLI engines to reduce viscous drag over the fuselage. However, the structure and control system of the BWB aircraft would be very complex. Furthermore, the seat layout inside the body would make rapid emergency egress very difficult and limit turnaround times. There is also little scope for easy extension and shrinking for family development.

2.3.5 Concept E: Strut-Braced Wing

Concept E was a strut-braced high-wing aircraft with a V-tail and underwing engines. The very high aspect ratio supported by the wing struts would significantly reduce the induced drag of the aircraft, and hinged wingtips would help alleviate gust loads through the wing. The underwing engines would be easily accessible and produce less cabin noise, although they would need long landing gear to provide suitable ground clearance. Although implemented to reduce the empennage surface area, associated control issues with a V-tail would require upscaling of the tail area, limiting or eliminating any benefit.

2.3.6 Concept F: High-Wing, T-Tail

Concept F had a high-mounted wing and a T-tail with wing-mounted engines. The high position of the wing would allow for shorter, lighter landing gear, although integration of the wing and landing gear with the fuselage would be heavy. The T-tail would produce predictable elevator response at the expense of added structural weight and the risk of deep stall at high angles of attack. The implementation of hinged wingtips would help alleviate gust loads at the expense of weight and complexity.

2.3.7 Concept G: Three Engine

Concept G explored the possibility of two wing-mounted engines and a third mounted inside the vertical tailplane. The third engine would provide additional OEI performance at the expense of increased fuel consumption and a weight penalty, each of which directly contradicts the key design driver. However, the wing's large aspect ratio would lower the induced drag of the aircraft.

2.3.8 Concept H: Oblique Wing

Concept H was an oblique wing aircraft with a T-tail and fuselage-mounted engines. The oblique wing would produce good drag characteristics throughout the flight profile, with a swept wing in transonic cruise and an unswept wing in slower parts of the mission. However, the oblique wing would be complex both structurally and in terms of aircraft control. The T-tail would increase the weight of the aircraft but have clean elevator onset flow. Rear-mounted engines would allow for shorter, lighter landing gear, though they would also increase cabin noise and they are harder to access for maintenance.

2.3.9 Down Selection

The eight concepts were evaluated against a set of pre-determined, weighted criteria using the Pugh Concept Selection Method, selected for its effectiveness when comparing concepts that are not refined and analysed enough for detailed comparison using calculated values. A combination of the requirement specification and engineering judgement led to the identification of important factors to consider in the design and marketability of the aircraft. Consideration of each criterion's influence on the key design drivers and impact on the economic viability, design timeline and system complexity determined weightings from 0 to 1 for each criterion. The concept designs were then decomposed into each criterion and compared against the Airbus A220 as a datum aircraft, chosen due to its similarity to the required design range, passenger capacity and environmentally conscious design philosophy. The team then scored each concept against the criteria with integer values ranging from -2 to +2. Positive and negative scores indicate that the concept met the criteria better or worse than the datum, respectively, while zero scores indicate relative parity with the datum. Table 1 shows the formulated Pugh scoring matrix with weighted and unweighted scores for each concept.

Table 1: Pugh selection matrix

CRITERIA	Weight	A	B	C	D	E	F	G	H
Fuel Burn	1	1	2	1	2	1	0	-1	1
Direct Operating Costs	0.8	-1	-1	1	-1	-1	0	-1	-1
Airport Operational Compatibility	0.8	0	-1	0	-2	-1	0	-1	-1
Operational Reliability	0.8	0	-1	-1	-1	0	0	-1	-1
Technical Maturity	0.7	0	0	-1	-1	0	-1	0	0
Safety	0.7	0	1	1	-1	0	0	1	1
Dynamics and Control Performance	0.6	0	0	0	0	0	1	0	-1
Complexity	0.6	0	-1	-1	-2	-1	0	-1	-1
Manufacturing Costs	0.5	0	0	-1	-1	0	0	-1	0
Family Development/Design Flexibility	0.4	0	1	0	-2	0	0	0	0
Aesthetics	0.4	0	-1	-1	-1	-1	0	0	-2
Noise	0.3	0	-1	-1	-1	0	0	-1	-1
Capacity	0.1	1	1	-1	2	0	0	0	0
RAW SCORE		1	-1	-4	-9	-3	0	-6	-6
WEIGHTED SCORE		0.3	-0.5	-0.9	-5.6	-1.6	-0.1	-4.1	-3
RANK		1	3	4	8	5	2	7	6

Due to the subjective nature of using engineering judgement and experience to weight and score criteria and concepts, the team decided to carry out a sensitivity analysis on the results. The analysis involved varying each weighting by ±20% and recalculating the concept rankings, indicating that the Pugh method gave robust results as the chosen concept remained the best choice regardless of weighting variations.

2.4 Subsequent Iterations

2.4.1 Seat Layout

Following the preliminary design phase, the cabin layout required a redesign to comply with CS-25.809 requirements. This also provided an opportunity to improve features related to turnaround time. Two overwing exits were added and Type B emergency exits replaced the Type C exits at the front to reduce passenger loading time. The results of these changes were a cabin that no longer fit within the fuselage. Two solutions were identified: increasing the fuselage length or changing to a five-abreast layout. The latter was selected for several reasons. Firstly, an informed [3] reduction of the fuselage wall thickness allowed the cabin floor to be raised but still fit the five-abreast seating without increasing the external fuselage diameter, improving turnaround time by granting additional height and volume for baggage handlers in the hold. Secondly, the five-abreast layout allowed longitudinal repositioning of the passengers' CG onto 25% MAC to improve the

aircraft's loaded CG position. Finally, increasing the fuselage length would have impacted the parasite drag and mass of the airframe, increasing fuel burn. Figure 6 shows the cabin seating changes implemented.

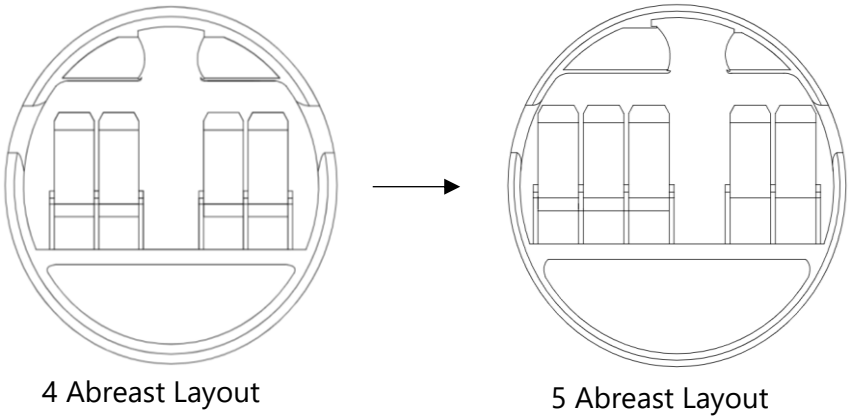

Figure 6: Cabin cross-section change

2.4.2 Mach number

While the initial concept had defined a cruise profile of 0.65M at 35000ft, this was primarily based on an attempt to empirically estimate the optimal profile to combine the low SFC capabilities of a high BPR turbofan and an aerodynamically efficient aircraft optimised for induced drag reduction. However, this was identified as a key design decision that would have a significant impact on fuel burn and aircraft design in later stages. A detailed trade study using resized wings and engines was thus carried out to find the altitude and Mach number that produced the highest SAR, and therefore the lowest block fuel. Figure 7 shows the results of this analysis, with the best cruise profile found to be at 0.67M and 35000ft.

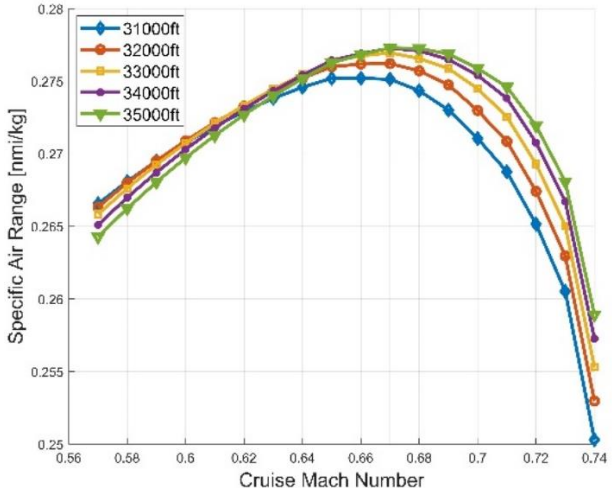

Figure 7: Study of SAR variation with cruise profile

3 Finalised Concept

3.1 Aerodynamics

The wing was initially sized based on the preliminary MTOW estimate and the requirement specification's mission phase constraints. These were translated into a constraint diagram that assessed the wing and thrust loading relationships for each phase to produce an allowable region of engine and wing sizing, shown in Figure 8. Selection of the aircraft design point focused on minimising thrust loading, to eliminate excess thrust and engine mass, and maximising wing loading, to mitigate parasite drag.

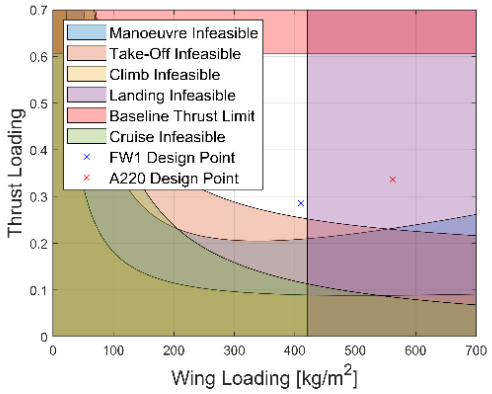

Figure 8: Thrust and wing loading constraints for each mission phase

A conservative wing loading of 410kg/m^2 was selected, allowing further development of the wing planform while ensuring design changes would not push the design point beyond the constraints. The AR of the wing is the most important factor determining induced drag and so was carefully analysed to find an optimal value. The analysis carried out assessed the wing weight implications of increasing AR and the fuel burn implications of lowering the induced drag factor. The SAR corresponding to different ARs was calculated through a similar study to that in 4.2.4, producing Figure 9, which indicates that increasing AR up to 20 maximises fuel efficiency.

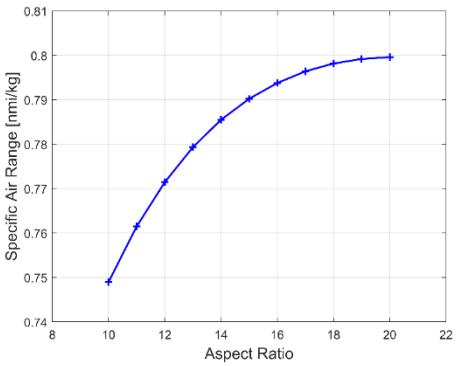

Figure 9: SAR variation with AR

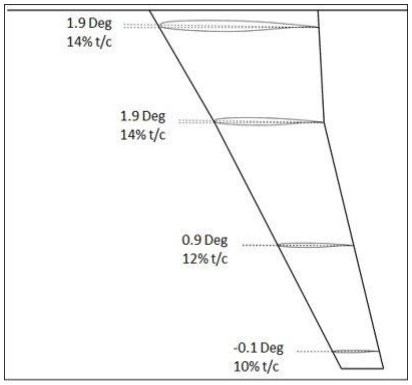

Figure 10: Aerofoil spanwise distribution

While this analysis indicated an optimal AR of around 20, the wing weight calculations used were designed for lower AR wings. Further research [4] into the problem demonstrated that, when more sophisticated, non-linear effects are considered, the optimal AR for a single-aisle passenger aircraft designed to minimise fuel burn is closer to 18, so this was selected. Combining this with the required wing area of 109m^2 produced a wingspan of 43.8m, which falls within the ICAO Code D requirement.

The aerofoil family was selected from the transonic cruise profile (0.67M, 35000ft) and the corresponding CL of 0.49. The supercritical NASA SC(2)-04xx aerofoil family met this condition well and had good stall and high-lift characteristics. An analysis of thickness implications on wing structural mass, parasite drag and, ultimately, fuel burn led to the selection of 14% thickness aerofoils for the wing kink, tapering to a 10% thickness aerofoil at the tip. The relatively large thicknesses of these aerofoils are also beneficial for flutter characteristics of the wing, which is a technical challenge posed by the high AR chosen, although in-depth analysis of aeroelastic characteristics goes beyond the scope of this project. Wing twist was then considered both for optimising the spanwise lift distribution and ensuring stall would begin at the root, aiding recovery. The resulting distribution of aerofoils, thicknesses and incidence angles are presented in Figure 10.

The high-lift devices for the wing were selected and sized based primarily on landing, take-off and MLG stowage constraints. The required CLmax of 2.4 was met using plain flaps of 20% chord distributed across the entire kink area. Consideration was given to the implementation of more sophisticated flaps that could increase the CLmax and thus decrease the area of the wing. However, fowler flaps and slotted fowler flaps tend to require a larger chord fraction, impinging on the tight restrictions for MLG stowage. Furthermore, the complexity of these flaps and the additional wing structure that would be required would increase the wing

mass. This issue is sensitive to the specifics of the stowage solution, wing sweep and high lift geometries and should therefore be re-evaluated during detailed design.

Though traditionally driven by maximising the aircraft's aerodynamic efficiency for the cruise condition over a specified mission, the MLG stowage constraints led to a compromised quarter-chord sweep of 13°. This produced a sufficiently large wing kink without a significant wing area increase while keeping a CG position sufficiently close to 25% MAC, reducing the weight penalty associated with wing sweep and mitigating the high AR aeroelastic effects that would be worsened by increasing sweep. The taper ratio of the wing was chosen to be 0.3 based on empirical data trends from [5] for maximising wing efficiency by approximating an elliptical lift distribution.

Figure 11 presents the drag polar of the wing planform, indicating an optimal L/D of 24.4. Due to compromises made for MLG stowage constraints, the actual wing L/D in cruise is 23.5. Despite the departure from optimal aerodynamic efficiency, the L/D is still better than all airliners for which data could be found. The A320, for example, sits at an L/D of around 16 [6].

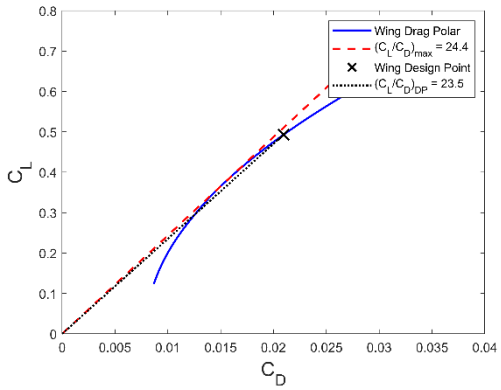

Figure 11: Wing drag polar

3.2 Operational Performance and Propulsion

Engine sizing considered many limiting cases and was ultimately driven by the time-to-climb requirement. To satisfy this, the baseline engine was scaled by a ratio of 0.94, yielding a static thrust of 63kN and a minimum cruise SFC of 0.5268 lbm/hr/lbf. Performance data for the engine was then calculated using the thrust change ratio and a correction to the SFC accounting for the change in blade size.

Table 2 lays out a breakdown of the aircraft's fuel consumption over the design and study missions. The block fuel for the study mission is 29% less than that of the Airbus A220-100 over the same mission [3].

Table 2: Mission fuel breakdowns

Mission Phase	Study Mission		Design Mission	
	Time [minutes]	Fuel [kg]	Time [minutes]	Fuel [kg]
Start-Up and Taxi Out	7	15	7	15
Take-Off	2	130	2	140
Climb	22	780	24	822
Cruise	40	660	115	1895
Descent	20	65	20	75
Approach	5	111	5	75
Taxi In	7	15	7	15
Block Total	103	1776	180	3073
Continued Cruise	45	715	45	685
Overshoot	2	95	2	95
Diversion	37	714	37	709
Approach and Landing	5	102	5	90
Reserves Total	89	1626	89	1579
Total	**192**	**3402**	**269**	**4652**

A common pylon structure was selected for engine attachment due to the conventional, underwing location of the engines. The spanwise position is 38% of the semispan; though further outboard than is conventional, this would aid the bending relief of the high aspect ratio wing. Furthermore, the vertical stabiliser and rudder were sized to meet OEI yaw balance and control requirements. Further discussion of the engine location is conducted in section 10.1. Thrust reversal capability is incorporated in the design to improve landing performance and satisfy requirements.

3.3 Materials and Manufacture

Most of the airframe (~60%) is to be constructed using CFRP sheets due to its high stiffness to weight ratio. This includes the skins and frames of the fuselage, wing and empennage. The black metal approximation was used for the design of the torque box, with isotropic material properties assumed as 3/8 of the unidirectional properties. Further analysis of the lay-ups for each component must be carried out in the detailed design stage. GLARE was selected for the leading edges of the wing and empennage, driven by its ability to withstand impact loads efficiently, reducing damage from small debris during take-off and landing. Titanium is still required in areas with high loading, such as landing gear connections, selected for its higher strength to weight ratio than steel that outweighs the additional cost, given the key design driver of minimum fuel burn.

The extensive use of composite materials may bring high initial manufacturing costs due to labour costs and expensive curing equipment. However, the benefits of composite materials were deemed sufficient to justify their use. Not only do composites significantly reduce the airframe weight by around 30% [4], thus fuel burn, but the long-term maintenance costs are generally lower. Composites have a high resistance to corrosion and fatigue and are less likely to be damaged by water. The use of adhesive bonding to connect individually cured parts also reduces the use of metal fasteners and allows a more evenly distributed stress field, reducing the likelihood of fatigue cracks appearing. An adhesively bonded joint is also smooth and clean, requiring less surface finishing, and requires less labour-intensive processing, such as assembly and finishing, driving manufacturing costs down.

3.4 Structural Design

The main wing is of a semi-monocoque structure with a twin-spar wing box design. The box is situated between 15 and 60% of the local chord and assumed to be symmetric, with spars 90% of the local aerofoil thickness, a common assumption used. The chordwise locations of both spars were chosen following general trends, such that the wing box is sufficiently thick and large to resist bending and torsion, respectively. The chordwise location of the rear spar provides sufficient space for control surfaces and landing gear stowage. For simplicity, the top and bottom skin panels were assumed flat in the analysis, producing an underestimation of the second moment of area.

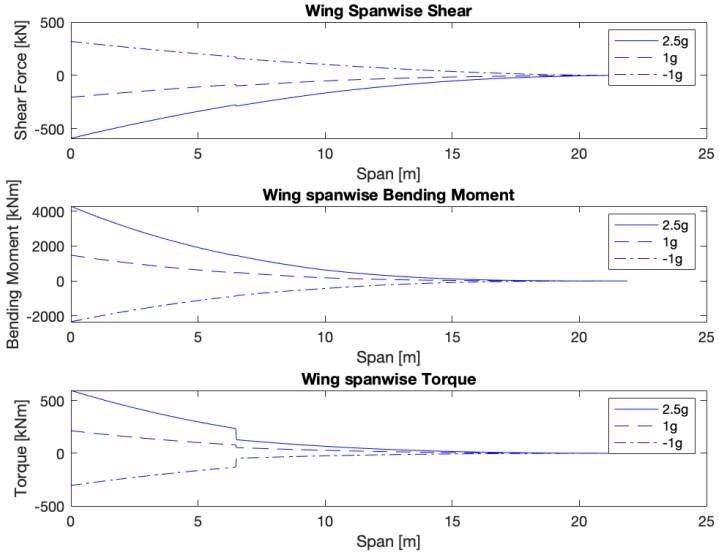

Figure 12: Spanwise structural load distributions

The area of the spar caps and thicknesses of the skins and webs were sized through consideration of the loads acting on the wing. Three key load cases were identified from the manoeuvre envelope (2.5g, 1g, -1g) and the

spanwise shear forces, bending moments and torque distributions were calculated, shown in Figure 12. Skin-boom analysis was used for sizing of the wing box, and the effects of stringers on the second moment of areas were accounted for using smeared skin thicknesses. Ribs were added to maintain the wing shape and withstand concentrated loads, such as landing gear loads, with their pitches sized with consideration of the stringer and resistance to spar column buckling. T-stringers were selected for their ease of manufacture and lower weight than z-stringers, another common type. The stringer pitches were sized through the calculation of the top skin panel buckling. A safety factor of 1.5 (CS25.303 [5]) was applied in all sizing calculations, the results of which are displayed in Table 3.

Table 3: Wing box sizing

Spanwise Location	**[% Semispan]**	**0**	**19**	**30**	**52**	**77**
Stringer Flange Thickness	[mm]	1.2	0.9	0.6	0.3	0.3
Stringer Web Thickness	[mm]	2.4	1.8	1.2	0.6	0.6
Rib Pitch	[mm]	639	749	885	1032	1032
Skin Thickness	[mm]	3.8	3	2.3	1.4	1.4
Stringer Pitch	[mm]	104	95.8	87.5	78.3	78.3
Smeared Skin Thickness	[mm]	7.6	6.1	4.7	3	3
Front Spar Web Thickness	[mm]	8.1	6.8	5.1	2.5	2
Rear Spar Web Thickness	[mm]	8.1	7.2	5.4	2.5	2
Front Spar Cap Area	[mm^2]	9000	8000	8000	6000	6000
Rear Spar Cap Area	[mm^2]	10000	9000	9000	7000	7000

To ensure the wing box is sufficiently stiff and that there are no major aeroelastic effects due to extreme deformation, the deflection and twist at the wing tip were found. Under the maximum load of 2.5g, the tip deflects 3.27m (17.2% semispan) with a twist of 5 degrees. This is slightly higher than similar aircraft, likely due to the higher aspect ratio, but is still of a reasonable level. The conservatism of this estimate should be noted, as the additional stiffness due to other components, such as the leading and trailing edges, were not included in the calculation.

The loads acting on the wing are transferred to the fuselage by the front and rear spars; therefore, the design of the connecting fuselage frames is very important. The principle of virtual work was combined with the assumption of ring frames to calculate the bending moment distribution around the frame for each load case, as shown in Figure 13. This allowed the calculation of the frame thicknesses for each spar. This resulted in a front frame thickness of 0.298m and a rear frame thickness of 0.306m.

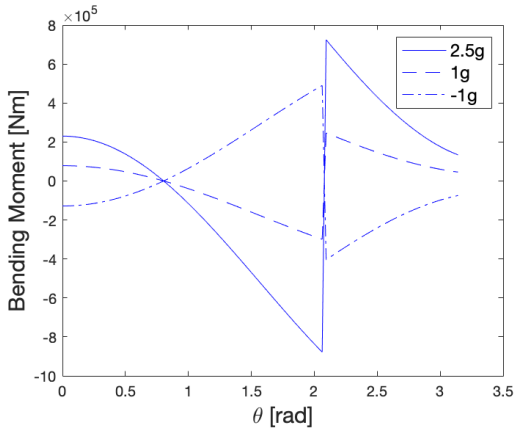

Figure 13: Bending moment distribution of half-fuselage ring, with θ measured clockwise from the top centreline

3.5 Weight, Balance, Stability and Flight Control

To aid the design process, a weight book containing component masses, CG locations and moments of inertia was constructed and maintained, facilitating in-flight and ground balance checks. Initial airframe and fixed equipment component masses were calculated using the averaged results of semi-empirical equations from Roskam [6], Torenbeek [7] and Sadraey [8], all of which were based on an initial MTOW estimate and

aircraft geometry. These were then combined with the turbofan propulsion system, design mission fuel mass, operator's items and payload masses from the requirement specification to produce the first iteration of MTOW. This process was iterated until convergence to a final MTOW was achieved. Any changes made to the aircraft in the iteration loops were incorporated through repetition of this approach. Major design decisions such as the majority composite construction and high aspect ratio wing were reflected in the weight book by the application of scale factors based on research data [4] [9]to affected component masses. Overall conservatism factors were also applied, as per the requirement specification, resulting in a final weight breakdown detailed in Figure 14.

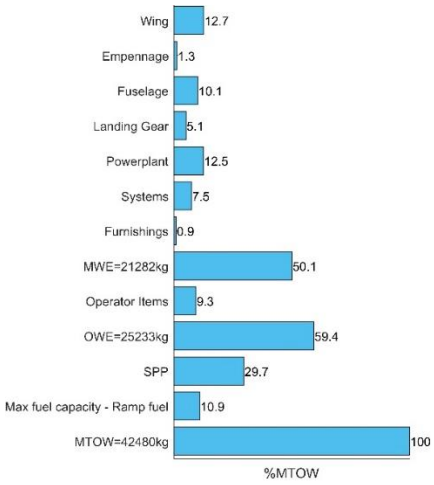

Figure 14: Aircraft weight breakdown

The CG locations of components, fuel and payload were similarly calculated using semi-empirical methods from [8], [6] and the aircraft's geometry. This allowed the production of the loading diagram presented in Figure 15 and analysis of the aircraft's ground and in-flight balance. The mostly conventional layout of the aircraft allowed its CG at SPP and MTOW to be positioned close to 25% MAC, with a slight adjustment of cabin and systems positions, helping to minimise trim drag. A trade-off between loading restriction and the required sizing of the horizontal tailplane for take-off rotation resulted in a 'windows-then-centre' loading policy that keeps the empennage mass reasonably low and produces a 29% MAC CG range. It should be noted that this decision was also affected by the restriction in MLG position, which meant that the 2.5% MTOW minimum NLG load limit was the critical aft CG case and the ability to rotate at take-off dictated the forward limit in ground balance.

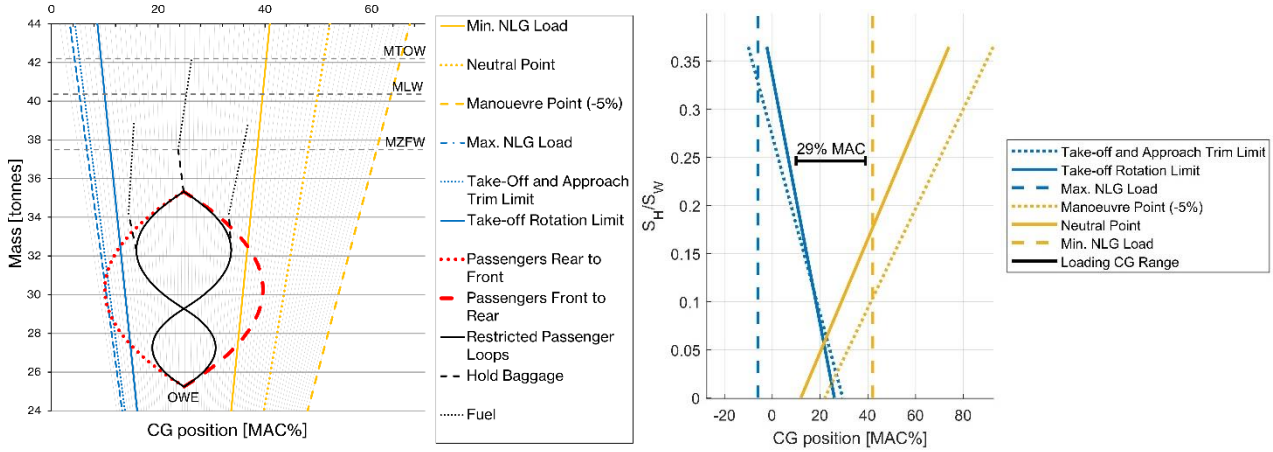

Figure 15: Aircraft loading diagram

Loading calculations and modifications were performed simultaneously with stability calculations to ensure the empennage and control surfaces met the requirements. The horizontal tailplane and elevator were sized according to, and checked against, the following:

- **Take-off Rotation**: the critical sizing case that ensures the aircraft could rotate around the MLG at MTOW with an appropriate angular acceleration of $4°/s^2$ [8].

- **Longitudinal Manoeuvre Stability**: Definition of the manoeuvre point, the furthest rearward the CG can travel during pitch manoeuvring before the aircraft no longer demonstrates restoring aerodynamic stiffness. A -5% MAC factor is added following Airbus' design approach [10].
- **Longitudinal Trim**: The moveable HTP must be able to trim the aircraft in all flight conditions, as defined in CS25.161 [5].

The Vertical Tailplane and Rudder were sized according to, and checked against, the following requirements:

- **One Engine Inoperative Control:** The critical sizing case due to the unconventionally outboard engine position. The rudder must be able to control the aircraft during flight in an OEI condition, as defined in CS25.149,161 [5].
- **Crosswind Landing Control:** The rudder must control the aircraft in crosswind sideslip conditions, as defined in CS25.177 [5].
- **Directional Static Stability**: Definition of the directional neutral point, the furthest rearward the CG can travel before the aircraft no longer demonstrates directional restoring aerodynamic stiffness, as defined in CS25.177 [5].

Roll rate calculations revealed that implementing empirically sized ailerons would not grant the roll rate required in CS25.147 [5] due to the aircraft's large span, which grants it high aerodynamic damping in roll and a greater rolling moment of inertia. Therefore, spoilers were conservatively sized and added to the design so that the aircraft met the requirements.

The aircraft employs a *more electric* control actuation system where all control surface deflections are activated by electrical signals from the flight deck that drive EHAs or EMAs running on bleed power from the engines. The primary benefits of these actuators are increased energy efficiency and reduction in mass over a fully hydraulic system, which will contribute to reducing fuel burn [11]. Specifically, EHAs will be used for the elevators, ailerons, spoilers and rudder. EMAs will be used for the flaps and trimmable HTP, where their demonstrated potential to jam [11] will not produce a safety risk. Secondary benefits of these power-by-wire actuators include easier and less frequent maintenance, reducing DOCs, and better dynamic characteristics than an all-hydraulic system.

3.6 Landing Gear

A tricycle landing gear layout was selected for its good stability characteristics and pilot visibility, with dual wheels for redundancy. Two MLG legs are positioned 17.65m rearward of the datum, behind the aft CG position, while the NLG is 5.4m rear of the datum. The wheel track is 6.36m, resulting in a turnover angle of 50.3°, which is within the 63°limit. Under the MTOW ground loading case, with the CG located 16.85m aft of the nose datum, the MLG carries 93.4% of the loading and the NLG carrying the remaining 6.6%. A nose steering angle of 75° gives the aircraft a turn width of 21.08m and gives a runway clearance larger than 4.5 m, giving compatibility with ICAO Code D. The LG height provides an engine clearance of 23% fan diameter when loaded and a tail scrape angle of 14.6°. While airborne, the MLG main fitting length is 2.65m and the NLG length is 2.29m. The MLG shock absorber piston diameter is 0.155m with a stroke length of 0.58m, requiring the main fitting diameter of 0.21m [12].

COMFAA 3.0 software [13] was used to calculate the aircraft's ACN value, giving 21.1. Several loading cases were considered during tyre sizing, including CS 25.491,493,495 and produced MLG sizes of 36x11.0R18 and an NLG size of 23.5x8.0R12. Carbon brakes were chosen for their lower weight and better energy absorption than steel [14], with sizing such that the brakes fit within the rim size and the space between the wheels.

The MLG retracts inboard into a cavity between the forward and aft cargo holds, whereas the NLG retracts forward into the fuselage. The MLG does not have full gear doors, rather the wheels are left open and flush with the lower surface of the fuselage and have aerodynamically faired hubcaps and carbon seals, much like the Boeing 737 [15]. This decision resulted from a trade study considering the drag increase of the uncovered wheel versus that of a larger bulge to accommodate the MLG and door plus the increased weight of the door. Figure 16 displays the landing gear in its deployed and retracted positions, with a clearance of 0.08m between the spinning wheel and aircraft structure. An electro-hydrostatic actuation system is employed due to its efficiency and redundancy advantages [16]. Also, the probability of jamming is much lower than that of an electro-mechanical system. The total weight of the MLG is 1197kg (without the EGTS) and the NLG weighs in at 250kg.

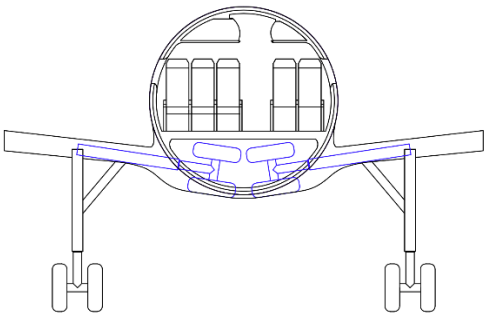

Figure 16: MLG stowage diagram

3.7 Fuel Systems

Two identical fuel tanks are incorporated in the wing, providing a total volume of 5.97m^2 and enabling carriage of the maximum fuel capacity of 4652kg. The tanks are positioned outboard of the engines, providing bending relief and allowing gravity feeding through the dihedral angle. Also, the position means that an engine disc burst situation would not damage the fuel tank, thus no dedicated dry bay is needed to mitigate fire risk and allow feeding to the operable engine through the cross-feed line. Vent tanks are included outboard of the main fuel tanks, allowing excess fuel and pressure to be withdrawn, maintaining constant tank pressure. A jettison system is not incorporated as the aircraft requires very little fuel burn before reaching MLW. There are fuel shut-off valves for the engines that stop feeding during an engine fire or OEI event and boost pumps ensure a constant positive feed pressure. The cross-feed valve and pump are positioned at the lowest point in the tank so that the maximum quantity of fuel is useable. Each wing's refuel panel has a single nozzle that links to the cross-feed line by additional plumbing. The refuelling time is estimated to be 6 minutes, using a standard refuel rate. Figure 17 outlines the fuel systems integrated with the aircraft design.

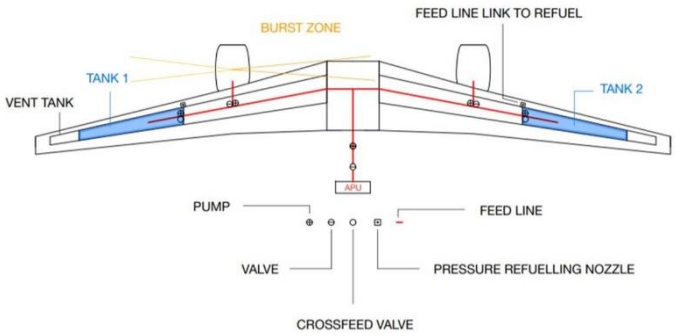

Figure 17: Aircraft fuel system layout

3.8 Aircraft Cabin Layout

Two cabin layouts were designed, a five-abreast high-density single-class arrangement and a four-abreast two-class configuration. The former was designed first and used as a basis for fuselage sizing to maximise the cabin's volumetric efficiency and minimise the fuselage wetted area and diameter, improving both the weight and drag of the aircraft. Included alongside the 120-passenger capacity were attendant seats, emergency exits, trolleys and lavatories, designed to meet the requirement specification and CS25 regulations. The resulting cabin is 22.8m long and 3.1m wide. The balance characteristics of the aircraft were also considered during the cabin design process, resulting in the centre of the seating area being located at 24% of the wing MAC.

The two-class layout was then formulated to fit within the existing fuselage constraints, giving capacity for 7 first-class and 72 second-class seats, 79 in total. The drastic reduction in capacity comes down to the increased aisle requirement for a two-class layout over the high-density arrangement, from 19 to 23 inches, and led to the economy-class rows becoming four-abreast. Despite reducing the marketability and increasing the two-class DOCs of the aircraft, the drag implications of facilitating a five-abreast two-class layout were deemed unacceptable as they would increase fuel burn. Further investigation into possible solutions that allow a five-abreast two-class layout without significant drag effects should be carried out in future design stages, such as a top-heavy fuselage cross-section.

3.9 Alternative Technologies Impacting Noise and Emissions

To best fulfil the key design driver of minimum fuel burn and improve compliance with current and forecast restrictions on noise and emissions, a range of novel technologies have been identified and analysed. Many EU-funded projects, such as OPERAIR, CLEAN SKY, COSMA and NACRE [16] were investigated to identify possibilities and several technologies were then selected for integration with the baseline aircraft design based on their efficacy, ease of integration and TRLs.

3.9.1 Noise Technologies

Table 4 lists the noise-reduction technologies that were considered, their associated TRLs and their likely availability dates.

Table 4: Noise reduction technologies

Technology	TRL	Likely Availability
Chevron Nozzles [17]	9	Available
Acoustic Liners [18]	9	Available
Noise Control Suppressor Nozzle [19]	7	Available
Toboggan Fairings [20]	6	2024
Ultra-High BPR Turbofans [21]	6	2028
Geared Turbofans [22]	6	Available
Internal Vanes, External Wedges [23]	4	2025
Flap Side-Edge Fences [24]	2	2030
Porous Flap Edges [25]	2	2030
Flap Edge Brushes [26]	2	2030
Flap CML [27]	2	2030
Plasma Actuator [28]	2	2035
Air Blowing and Suction [29]	2	2030

For noise reduction of the baseline aircraft, chevron nozzles and acoustic liners were selected for their high TRLs and likely availabilities before the 2027 EIS requirement. Chevron nozzles are a mature jet noise reduction technology that uses the geometry of the nozzle to smooth the mixing of the exhaust and bypass flows, reducing turbulence in the jet [30]. These nozzles can reduce A-weighted jet noise by an average of 1dB and, although they slightly lower the engine's thrust, their shape can be tuned to optimise the noise-thrust compromise [17].

Acoustic liners consist of a lightweight layer of noise-damping composite materials embedded in the nacelle wall and can reduce engine acoustic energy by 20-30dB using Helmholtz's resonance principle [31]. Acoustic lining can also be integrated into the fuselage wall to reduce the cabin noise levels.

Noise control suppressor nozzles were rejected due to the associated engine redesign and manufacturing difficulties. As the only other technology that is likely to be suitable before the 2027 EIS date, toboggan fairings were also considered as they are effective at reducing noise due to turbulent flows around the landing gear. While the low weight and cost implications initially were encouraging, research [32] suggested that there can be significant issues with brake cooling, tyre deflection and steering mechanism interference that make their integration difficult.

As the project is constrained to the use of the provided turbofan engine, the ultra-high bypass ratio and geared turbofan engines cannot be implemented within the scope of this project. However, their implementation should be considered in further design stages for their improvements in both noise and carbon emissions.

The assignment of turbofan engines and the low TRLs of the other identified technologies led to their rejection for the aircraft, as the requirement specification would no longer be met. However, the design features under-wing engines, which provides passive damping of engine vibration along the wingspan, aiding cabin noise reduction [33].

3.9.2 Carbon Emission Technologies

Beyond the overall optimisation of the design to minimise drag and fuel burn, an electric green taxiing system (EGTS) was considered to reduce ground-level emissions. The EGTS uses battery-powered motors to drive the MLG wheels for taxiing in and out, allowing the engines to remain off until the aircraft reaches the runway, albeit at the expense of added weight. The other taxiing option considered was to use ground crew to start the engines, omitting an APU as they are heavy, polluting and inefficient. A detailed study into the weight and, ultimately, fuel burn implications of the combined EGTS and APU configuration was carried out, finding the fuel burn changes for each mission phase. The study concluded that the implementation of the EGTS and APU would save 124kg of fuel over the study mission and 110kg over the design mission, therefore the EGTS was introduced into the design.

3.9.3 Aircraft Noise Emissions

Estimation of the aircraft's community noise levels was carried out using a simplified noise method [34], which was then compared to ICAO limits to find the cumulative margin. Table 5 outlines the results of these calculations.

Table 5: Aircraft noise levels

Effective Perceived Noise	Baseline [dB]	ICAO limit [dB]	Margin [dB]
Sideline	92.5	94.7	-2.17
Approach	96.1	98.7	-2.52
Flyover	82.5	89.0	-6.47
Cumulative	271.1	282.4	-11.16

Table 5 shows that the design meets ICAO certification requirements with a cumulative margin of 11.16dB and all local margins greater than 2dB. The London-Heathrow quota count targets are also met, with the aircraft classifying as 0.5 for both departure and arrival. However, the target of ICAO Chapter 3 minus 25EPNdB has not been successfully met. This may impact the future marketability of the aircraft if noise regulations tighten, therefore, further work should be carried out on reducing the noise emissions of the aircraft.

Cabin noise was estimated through the calculation of the external sideline noise level at ICA, producing a value of 86.7EPNdB. It should be noted, however, that these calculations again consider neither the chevron nozzles and nacelle acoustic liners nor the fuselage acoustic lining. Estimations of these effects indicate a worst seat noise level of 66.7EPNdB and an average of 61.7EPNdB.

3.9.4 Aircraft Pollutant Emissions

Lack of sufficient data corresponding to the provided turbofan engine led to an estimation of NO_x emissions through research into engines with similar thrust ratings in the ICAO 2020 emission databank [35]. The CF34-8E5A1 engine was identified as the most similar and produces average NO_x emissions of 38.71g/k N at a pressure ratio of 24.12. The ICAO standards [36] for an engine of the same pressure ratio give a CAEP6 limit of 47.26g/kN. This is higher than the estimated NO_x emissions of the CF34-8E5A1, indicating that the designed aircraft would likely also fall within the limits.

4 Aircraft Characteristics vs. Requirement Specification

Table 6 lists the primary requirements from the specification, categorises them as either hard or soft requirements and details the aircraft's fulfilment of the requirements. Hard requirements are those that were deemed vital for the aircraft's success while soft requirements were less important, and their outcomes resulted from other design decisions. All the requirements were successfully met and the section below Table 6 outlines how the aircraft satisfies each of them.

Table 6:Analysis and satisfaction of specified requirements

Requirement	Unit	Hard/Soft	Target	Aircraft	Code
High density passenger capacity	pax	Hard	120	120	A
Low density passenger capacity	pax	Soft	Result	79	B
Design range with high density capacity	nmi	Hard	1000	1000	C
Study mission	nmi	Hard	500	500	D
Cruise speed	Mach	Soft	TBD	0.67	E
Time to climb (1500ft to ICA at ISA)	mins	Hard	≤ 25	24	F
Maximum cruise altitude	ft	Soft	TBD	36400	G
Approach speed (MLW, S-L, ISA)	kts CAS	Hard	≤ 140	125	H
Take-off Field Length (MTOW, S-L, ISA+15)	m	Hard	≤2000	1865	I
Landing Field Length (MLW, S-L, ISA)	m	Hard	≤1600	1558	J
One Engine Inoperative Altitude	ft	Soft	Result	16000	K
VMO / MMO	kts CAS/Mach	Soft	As calculated	350/0.96	L
Equivalent Cabin Altitude	ft	Hard	8000	8000	M
Turn-Around time	mins	Soft	Result	30	N
Airport compatibility limits	-	Hard	ICAO Code D taxi and gate	Met	O
DOC target	$/seat nmi	Soft	Result	0.184	P
Engine availability	Year	Hard	2027	2027	Q

A. The cabin layout in Figure 1 details a high-density seat layout capable of seating 120 passengers.
B. The two-class layout resulted from the fuselage and cabin size formed from the high-density arrangement. The proportion of first-class and second-class seats was determined through market research and a maximum provided in the specification. Changes also needed to be made to aisle width, seat pitch and seat length, producing a configuration that provides seven first-class and 72 second-class seats, 79 in total.
C. The aircraft had to be able to carry the high-density payload over 1000nmi. The amount of fuel necessary was calculated using a Breguet range-based performance code and given aircraft parameters for this hard requirement to be met.
D. The study mission is more representative of typical mission lengths and is used for the fuel burn and financial comparisons with competitors. The aircraft achieves a fuel burn 29% less than that of the A220-100 over a 500nmi journey.
E. The cruise Mach number was selected based on a trade study analysing several engine sizes, altitudes and cruise speeds, with each iteration using a new aerodynamically optimised design. The cruise profile yielding the highest SAR, and thus the lowest fuel burn, was selected.
F. The aircraft was required to climb from 1500ft to ICA within 25 minutes. This, along with the minimum fuel burn driver, led to the selected engine size and produced a time to climb of 24 minutes.
G. The aircraft's ceilings are defined by the rates of climb at that altitude. The service ceiling of this aircraft is the highest altitude at which a maximum rate of climb of 100ft/min can be achieved, corresponding to 38500ft. The absolute ceiling has a maximum rate of climb of 0ft/min and was found to be 39500ft whereas the maximum cruise altitude requires a maximum climb rate of 300ft/min, achievable at 36400ft.
H. To achieve a sufficiently low approach speed to come to a halt within the required field length, high-lift devices were used to lower the stall speed of the aircraft and allow an approach speed at MLW of 125kts.
I. The take-off field length was deemed a hard requirement as it is based on airport compatibility. With the engine size driven by climb requirements, there was enough thrust to take-off well within the required field length. This allowed lighter and less sophisticated high-lift devices.
J. Similarly, the landing field length was a hard requirement. A safety factor of 1.66 was applied to the calculation results to account for pilot and handling qualities. The aircraft can land within the given field length on a dry runway. On a wet runway, the aircraft needs to use thrust reversal.

K. The OEI ceiling results from the engine size and aircraft mass and is calculated with consideration of windmilling and asymmetric drag at the aircraft's minimum drag speed. The ceiling was found to be 16000ft, which would preclude the aircraft from flying over many mountainous regions.
L. As no specific values were required for VMO and MMO, they were deemed soft requirements and the structural qualities of the aircraft allow operation at up to 350kts.
M. Though no specialist has focused on the avionics and systems within the aircraft, assumptions have been made for the fulfilment of related requirements and the increased weight and cost of these systems were approximated using empirical data and accounted for in relevant calculations.
N. As the turn-around time was specified as a design result, it was deemed a soft requirement, though consideration was given to the fact that minimising it improves the financial viability and utilisation of the aircraft. Based on empirical data, the time was estimated to be 30 minutes. The size of the cargo bay was an important consideration for this, and the fuselage dimensions had to be modified from the preliminary design to allow easier baggage handling. Baggage handling is manual and there is no facility for use of containers.
O. For airport compatibility reasons, the requirement for ICAO Code D compatibility was deemed a hard requirement. This sets a maximum wingspan of 52m and wheel span of 14m, both of which are met by the aircraft.
P. Though traditionally the key driver, the DOCs were a secondary consideration given the importance of minimising fuel burn, so they were assigned as a soft requirement. The conventionality, low fuel burn and high utilisation of the aircraft produced DOCs of 18.4cents per seat nautical mile, less than the 20.4cents per seat nautical mile estimated for the A220-100 for the same mission.
Q. As the aircraft's engine is simply a scaled version of the baseline, non-geared turbofan engine, albeit with chevron nozzles, it was assumed that the provided engine would satisfy the 2027 availability requirements.

5 Zero Carbon Emission Variant

To eradicate the carbon emissions of the aircraft, a full redesign of the propulsion and fuel system was required, as no kerosene-burning solution is acceptable. After research into possible solutions, three were identified for detailed research, analysis and consideration (nuclear power was also considered but instantly rejected for its very low technology level and massive safety implications). Table 7 documents these options, their TRLs and their predicted availability dates.

Table 7: Zero-emission propulsion options

Technology	TRL	Likely Availability
Hydrogen Combustion	6	2027
Hydrogen Fuel Cells	5	2030
Battery Power	4	2028

The battery-powered and hydrogen fuel cell solutions are both *true zero* solutions, that is there are no GHG emissions whatsoever, but they were rejected for their weight implications and technology readiness levels, respectively. Batteries also have high risks of fire or explosions due to overheating during high-power or extended use, creating additional safety risks. While hydrogen fuel cells have the highest fuel efficiency (30% more than hydrogen combustion [37]) and the lowest noise levels, they also have a low TRL and would require the most drastic airframe redesign.

Liquid hydrogen combustion, on the other hand, can be implemented with little redesign as kerosene-burning engines are relatively easily modified. While not a *true zero* solution, the requirement for zero carbon emissions would be met with hydrogen combustion. Furthermore, the high energy density of hydrogen means that less fuel mass is required for the same mission profile [37]. Though the TRL of hydrogen combustion is only 6, due to issues with cryogenic containment of the fuel, there is a large volume of research being carried out in this area, indicating that viable solutions may be available by 2027. This led to the selection of hydrogen combustion as the zero-emission variant's fuel system. It should also be noted that the combustion temperature of hydrogen is higher than that of kerosene, which may produce more NO_x emissions than expected from a conventional turbofan engine. Additionally, steam is a by-product of the reaction and would form visible, but rapidly dissipating, clouds.

The low boiling point of hydrogen (20.35K), means that the fuel can easily boil-off into its very flammable and low-density gaseous form. To combat this issue, sophisticated pressurised cryogenic storage tanks with insulated walls are required. Furthermore, the low volumetric energy density of the fuel means that a large volume of hydrogen is required to fulfil its mission. The shape of the tanks is very important, as the surface area must be minimised to keep heat transfer, and thus boil-off, to a minimum. Spherical tanks are the most efficient shape for limiting heat transfer, though cylindrical tanks are also viable, albeit with a larger tank mass required [38]. As a result, fuel tanks within the wing box are not a feasible solution, and the fuel must be stored within the fuselage. External wing tanks were also considered, though the heat transfer and volume requirements would require massive, aerodynamically inefficient tanks.

To maximise the gravimetric efficiency of the hydrogen storage, spherical tanks should be used, and this approach was the first taken, with a tank placed aft of the rear pressure bulkhead. However, a spherical tank sufficiently large to store enough fuel would significantly increase the local fuselage diameter. A cylindrical tank of the same volume and an acceptable diameter was also deemed infeasible, as pitch stability analyses revealed unacceptable balance problems. The final configuration selected was a spherical tank behind the cabin with the same diameter as the inside of the fuselage and a cylindrical tank between the cabin and cockpit to store the remainder of the fuel. The front tank is of a low enough diameter that flight crew can walk beside it, meaning that additional doors and toilets for the pilots are not required. The resulting length increase of the fuselage is 6.5m and Figure 18 indicates the positions and sizes of these two tanks. This increase in fuselage length would allow for the same 120 seat passenger capacity as the baseline aircraft.

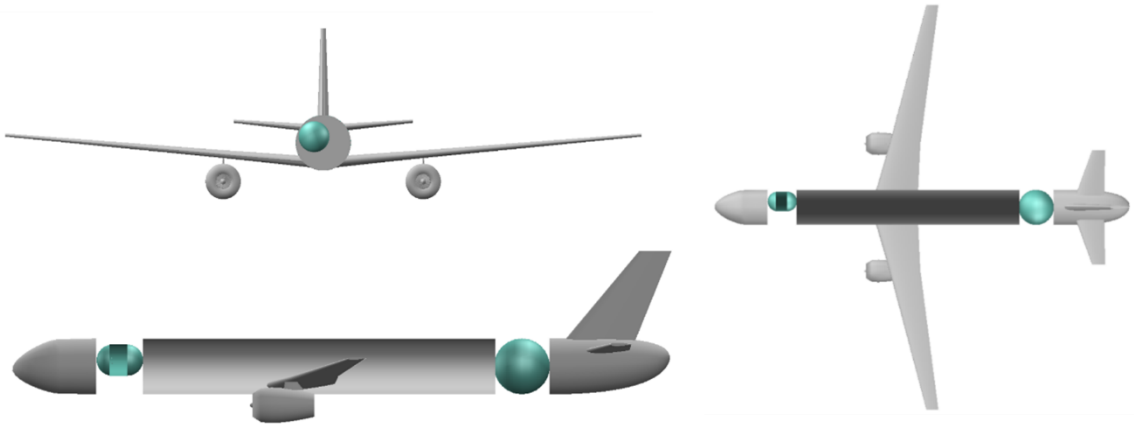

Figure 18: Visualisation of hydrogen tank locations and geometries, with approximate longitudinal wing placement

The split placement and uneven mass distribution of the two tanks at the ends of the cabin, rather than close to the MAC, would result in larger in-flight CG movements due to fuel burn, an issue that cannot be solved with fuel redistribution systems as commonly used in kerosene-burning aircraft. Therefore, a larger, heavier empennage would be required [38] to ensure acceptable trim capabilities over the larger CG range in all stages of flight. The possible weight increase may require a redesign of the wing planform to provide the additional lift. The aerodynamic performance would also be affected by the added fuselage length, which would increase the aircraft's parasite drag. The removal of fuel from the wing box would also impact the structural efficiency of the wing as there is no longer any bending relief. The wing structure would therefore need to be reinforced both to improve bending resistance and aeroelastic damping (due to the lower wing weight).

Due to the technical sophistication of the hydrogen storage tanks, frequent safety inspections should be required, which would increase the maintenance costs of the aircraft. The cost of fuel would be higher than that of hydrogen for several reasons. To fully satisfy the zero-carbon requirement, 'green' hydrogen (obtained by methods that do not release carbon) must be used, which is more expensive than kerosene. The infrastructure behind hydrogen fuel is also much less advanced than that of kerosene and the fuel would need to be transported in pressurised cryogenic tanks. Also, the cost of personnel training for safe handling and storage of hydrogen must be accounted for, which, when combined with the added fuel maintenance costs, increase the overall DOCs of the aircraft.

There are potential benefits associated with the implementation of hydrogen-burning engines that go beyond the removal of carbon emissions. Hydrogen burns much hotter and more quickly than kerosene, with a higher combustion efficiency, which can produce a smaller jet and allow for smaller, lighter engines.

6 Technology Levels and Risk Analysis

6.1 Engine Positioning

The position of the engines at 38% of the semispan was identified as a possible technical risk, requiring a larger vertical stabiliser. Conventionally, engines tend to be closer to 30% of the semispan, and for much lower aspect ratios. The positioning was driven by this high aspect ratio and the small fuel tanks, thus low wing weight, and the rib-reinforced wing structure at the kink. Though the vertical stabiliser is sufficiently large to offset an OEI condition, an in-depth trade study should be conducted to optimise the spanwise position of the engines, based on the resulting wing mass, tail mass and fuel burn for each position.

6.2 Composites

One of the issues related to the use of composites is low crashworthiness. Generally, composites are very brittle and undergo deformation more easily than Aluminium. Aluminium can sustain more than 24 times the deformation and can absorb energy 65 times more effectively than composites [4]. This creates the need to add additional structural support, especially for the fuselage, to allow it to withstand the same level of crashworthiness than metal alloys. Furthermore, although composites have great burn-through protection, pyrolysis of resin may produce toxic gases in the case of a fire. Aluminium frame spray is also required to provide electromagnetic shielding from lightning shocks.

Current established infrastructure for recycling metal alloys cannot be used for recycling composites. Most composite components ended up in landfills or incinerated when they reached their end of life. Currently, the main methods for recycling composites involved solvolysis or pyrolysis to dissolve the resin, leaving clean fibres that can be reused [40]. Even though only 10% of composites in the UK are being recycled [41], stringent legislation requiring composite recycling suggests that, by the end of the aircraft's service, more mature processes will have been developed.

6.3 Landing Gear Integration

The integration of the MLG proved a major design challenge given the high AR, low sweep and small root chord of the wing, resulting in a small wing kink chord. This challenge was identified at the end of the preliminary design stage, allowing subsequent design work to determine the geometry of the wing kink with a trade-off between aerodynamic performance and stowage space. At the end of each iteration stage, a cross-section from the updated GA, as in Figure 16, was used to ensure sufficient stowage space for the MLG within the kink and fuselage. Calculations were also carried out to ensure its location relative to the NLG and most aft CG location maintained a 2.5% MTOW ground load on the NLG.

6.4 Aeroelasticity

Another area of risk identified with the aircraft is associated with the aeroelastic characteristics of the wing. The large span and high AR of the wing pose possible issues with the aircraft's aeroelastic response, which may be worsened by the low mass of fuel in the wing, and therefore the low wing mass. However, these effects are mitigated by the low wing sweep and selection of relatively thick aerofoil sections. A simplified aeroelastic analysis of the aircraft with minimum fuel weight was carried out to find the wing's damping modes at different speeds, the results of which are shown in Figure 19. The calculated critical flutter speed was 0.97M, which falls within the CS-25.629 [5] requirement by 0.01M.

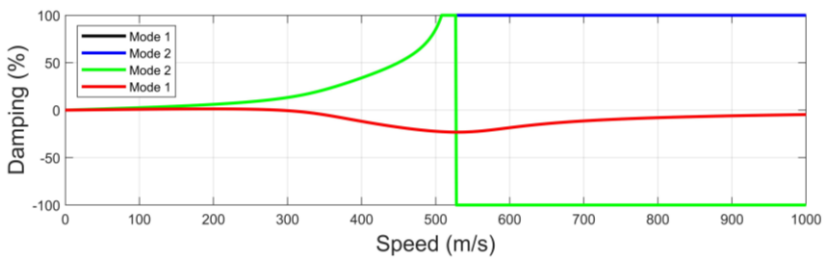

Figure 19: Analysis of wing aeroelastic damping

The removal of fuel mass from the wing structure in the zero-emission variant and towards the end of flight for the baseline, however, may push the critical flutter speed below the requirement. A more sophisticated analysis model should be applied to both design variants to ensure flutter requirements are met and addition of wing mass beyond the already-required structural improvements to the zero-emission variant may be required.

6.5 EGTS

As a less conventional aspect of the aircraft's design, the EGTS was deemed a potential risk in the effective integration of the aircraft's systems and the fuel efficiency of the airframe. The maturity of the EGTS was assessed by the ATNE specialist and a TRL of 8 was assigned to it. There was no risk of the technology not being sufficiently advanced by the EIS as it is already implemented on a range of aircraft. Though the analysis of the EGTS impacts on fuel burn proved it to be beneficial, integration of the motors and batteries with the MLG, considering the strict positioning, may become a challenge in future design phases.

6.6 Spoilerons

The larger-than-conventional span of the aircraft gives it greater aerodynamic damping in roll than comparable aircraft. Therefore, spoilers are implemented into the design to make up for the inability of outboard ailerons to provide enough roll power for the aircraft to meet CS25.147 [5]. The size of the implemented spoilers was chosen conservatively according to a research study [39]. However, since the addition of spoilers adds weight to the wing, to ensure fuel burn is optimised, CFD or wind tunnel testing to determine the minimum required spoileron mass should be undertaken in the next stage of design.

6.7 Hydrogen Fuel System

The primary technical challenge posed by the zero-emission variant is the storage of the hydrogen tanks. The pressurised, cryogenic storage requirements require sophisticated materials, structures and integration systems to prevent boil-off. While the tanks were initially sized based on empirical data for hydrogen storage, integration of these tanks into the airframe, as well as detailed definitions of their sizes, will likely be difficult. The tank configuration that has been selected, while initially appearing effective, may create significant, unpredicted problems that would require a drastic redesign of the aircraft. The health and safety implications of these tanks with regards to passengers, flight crew and airframe integrity have not been analysed and should be considered in detail in subsequent design phases.

7 Economic Analysis: Acquisition and Through-Life

7.1 Lifecycle Costs

There are several phases associated with an aircraft's lifecycle, including research and development, production and verification, utilisation and decommission. Each stage has an associated cost that must be considered when analysing the financial feasibility of a project, the sum of which is the total life cycle cost. A combination of several methods from [40], [6] and [41]were utilised alongside market research to estimate these costs.

The MSP was estimated by comparison of existing aircraft cost and passenger capacities sourced from manufacturers' websites and are presented in Figure 20. A trend was then drawn and resulted in an aircraft MSP of $60million.

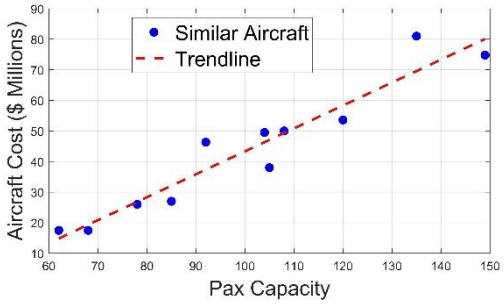

Figure 20: Market Study on MSP

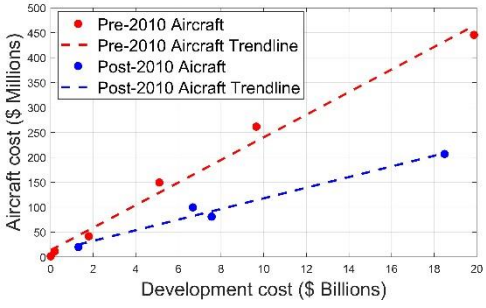

Figure 20: Market study on development cost

The development costs of the aircraft, also known as non-recurring costs, are related to the research and development phase of the aircraft lifecycle. Clear trends were identified among older and more modern aircraft (post-2010), indicating a higher development cost for the latter. This is likely due to increased design complexity and use of more sophisticated technology, such as composite materials or high BPR engines. A combination of the trend shown in Figure 21 and methods from [6] and [40] produced an estimated development cost of $3.73billion.

The manufacturing cost of the aircraft, related to the production and verification phase and sometimes called the recurring cost, was also calculated using a combination of market research and [6]. The estimated manufacturing cost per aircraft was estimated to be $37million.

The decommissioning cost was not calculated within the scope of this project. However, the most notable differences in design between the baseline aircraft and the A220 are the AR and sweep of the wing. These are unlikely to impact the decommissioning cost, indicating a similar cost to that of the A220. Further studies should be carried out regarding decommissioning, both for a more accurate cost calculation and a more in-depth analysis of the aircraft's environmental impact. This is especially pertinent due to the use of composite materials, which are difficult to fully recycle and thus may increase the lifecycle carbon footprint of the aircraft.

7.2 DOC Breakdown and Comparison

The DOCs associated with the aircraft were calculated using [41] and are broken down in Figure 22. The most significant contribution comes from the overall operating costs (49.4%), followed by in-flight costs (31.4%) and maintenance costs (19.2%). The financial costs are most closely associated with the aircraft utilisation and acquisition cost for the client. A high utilisation helps minimise DOCs, which can be achieved through optimisation of turnaround and flight times. The turnaround time of the aircraft was investigated and optimised through careful consideration of refuelling time (6mins) and a sanity check on the cargo bay size. This was carried out by creating a physical mock-up of the hold area to ensure loading and unloading would be sufficiently feasible. When this check proved sufficient space in the cargo hold, the turnaround time was assumed to be comparable to the A220. Fuel burn makes up more than 16% of the operating costs for the 500nmi mission, and it is clear to see that minimising fuel burn would improve both the aircraft costs and environmental impact.

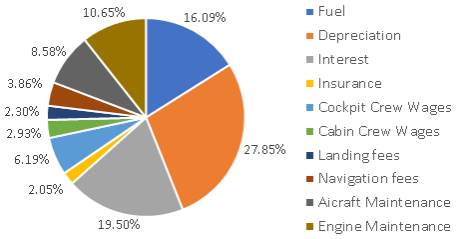

Figure 21: Breakdown of DOCs

The marketability of the aircraft is most clearly demonstrated through comparison of DOCs and COCs with a close competitor. The A220-100 was selected as the comparison aircraft due to in part to its similar size and technological sophistication, as well as the availability of its data. Table 8 demonstrates the reduction in these costs achieved by the aircraft.

Table 8: Aircraft cost comparison

Aircraft	**DOC** (cents/seat-nmi)	**COC** (cents/seat-nmi)
A220-100	20.4	10.4
Our aircraft	18.4	9.7
% change	-9.8	-6.7

7.3 Trade Studies and Sensitivity Analyses

Sensitivity studies were conducted to investigate the impact of changing market conditions on the DOCs and COCs of the aircraft. Figure 23 visualises the impact of variations in fuel price and MSP, indicating a large effect on COCs with fuel price and, by extension, fuel burn. The MSP variations are less significant as these are more closely related to acquisition costs.

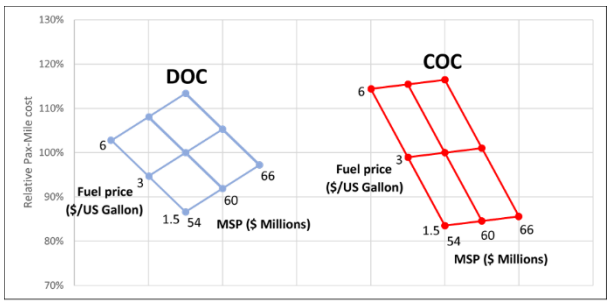

Figure 23: Sensitivity of costs to fuel price and MSP

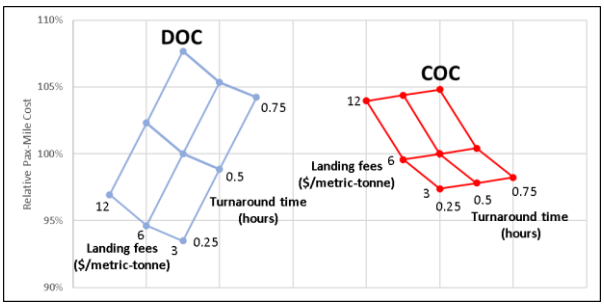

Figure 23: Sensitivity of costs to landing fees and turnaround time

The sensitivity of the DOCs and COCs to changes in turnaround time and landing fees were also analysed. Figure 24 shows these effects and highlights that COCs are more affected by landing fee changes, whereas turnaround time has a greater impact on DOCs. This is due to the utilisation of the aircraft increasing with reduced turnaround time, lowering the cost per flight and increasing client profits. Efforts to reduce turnaround time would therefore have extensive benefits to marketability and financial viability of the aircraft.

The impacts of cruise profiles on DOCs were also assessed, using the SAR results from the altitude and Mach number study detailed in 7.4.2. Figure 25 presents the results of this analysis, indicating that aircraft marketability would be maximised for a cruise of 0.73M at 31000ft. However, the importance of fuel burn outweighs the financial benefits of flying at this design point.

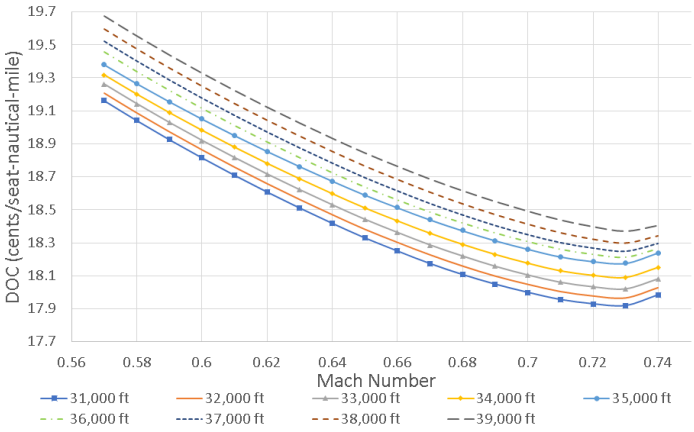

Figure 24: DOC variation with cruise profile

The quantitative effect of this decision is an increase in DOCs by 0.52 cents per seat-nautical-mile and an increase of $313 for the 500nmi study mission. Though not currently focused on client economic considerations, projected increases in fuel price and the global push towards carbon-neutrality may improve the marketability of the aircraft in the long term.

7.4 Manufacturer profitability

For the sake of this limited economic analysis, the acquisition price was assumed to be equal to the MSP, which resulted in a profit margin of $23million per aircraft. Figure 26 demonstrates an empirical trend in the MSP and breakeven number of aircraft, with a 50% uncertainty applied. Applying this trend to the baseline aircraft produces a breakeven number of 163. However, the acquisition price of aircraft tends to be much lower than the MSP, often due to price deals between clients and the manufacturer. This is likely to give a higher breakeven number than calculated using this model.

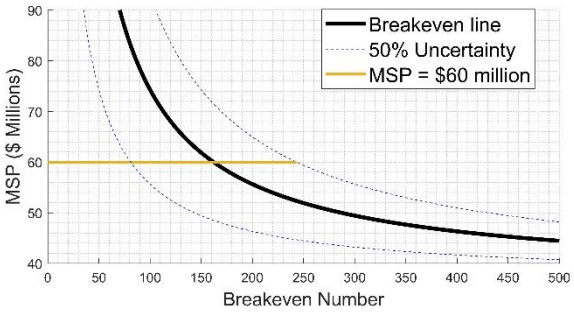

Figure 25: Breakeven diagram

8 Critical Analysis of the Design

8.1 Aerodynamics

The aircraft designed exhibits good aerodynamic efficiency, with an L/D of 23, where most competitors fall around the 19 mark. This can be primarily attributed to the optimisation of induced drag efficiency through the high AR wing and carefully considered planform characteristics. However, the focus on induced drag has led to a significant parasitic drag contribution. Wind tunnel tests and CFD analyses should be carried out over the aircraft to accurately assess local contributions and identify areas for geometric improvements. For example, interference fields at the engines and wing root could be optimised or different flap and wing area combinations could be analysed to alleviate the MLG stowage constraint. Additionally, technologies that help reduce viscous drag could be researched and analysed for integration in the design, such as LFC or shark-skin surface coatings. The aircraft would also benefit from further analysis of the aeroelastic characteristics of such a high AR wing to ensure CS25 requirements are safely met for both the baseline and zero-emission variants.

8.2 Operational Performance and Propulsion

The low fuel burn design of the aircraft is proven by its aforementioned 29% reduction against the A220 over the study mission. This can be primarily attributed to the low induced drag of the wings, the extensive trade study on cruise profiles and the implementation of an EGTS. To further maximise fuel efficiency, an investigation into the optimum climb speed should be carried out, as climb is a major contributor to fuel burn over short-range missions. Additional improvements could be implemented through in-depth research into engine-pylon structures to minimise parasitic and interference drag contributions.

8.3 Structures

The wing structure is sufficient to withstand the loads in the provided manoeuvre envelope, though time constraints prevented the consideration of gust loads in the design. Automated optimisation techniques should be applied to the structural design to minimise wing weight. Furthermore, analysis of the structure was only carried out at a few spanwise locations. Better results could be found using detailed FEA that predicts the linear deformation more accurately. Other structural components, such as the fuselage and empennage, should be sized in further design stages.

8.4 Weights, Balance & Stability

Within the scope of the analyses in this project, the aircraft meets all balance and stability requirements and the similarity of the tail volume to comparable aircraft suggests some validity. However, the sizing and positioning of the ailerons and spoilers lack in-depth understanding and further analysis, be it physically or using CFD, should be undertaken before the conclusion of the detailed design phase. The restricted MLG position also forced the adoption of a restricted loading policy to mitigate tail mass impacts. Additional analysis should be carried out into the loading policy's impact on aircraft marketability and turn-around time, providing better justification of the design decision or simply a more effective possibility.

8.5 Landing Gear

The landing gear design can carry the aircraft under various loading cases and integrate into the fuselage with sufficient stowage volume. To improve the definition of the landing gear design, detailed stress analyses over the fittings and bracing strut should be carried out. Weight estimations would then benefit from the more detailed design geometries and materials.

8.6 Aircraft Architecture, CAD and Systems

The driver for minimum fuel burn that led to a high-density single-class cabin layout with a maximised volumetric efficiency produced a cabin floor that perfectly fit the five-abreast configuration. The required increase in aisle width for the two-class layout led to a four-abreast economy class and a greatly reduced passenger capacity. While this was an intentional design decision to optimise the fuel burn of the high-density layout, it reduces the marketability of the aircraft. A detailed trade study could be conducted to look for solutions that would allow five-abreast economy seating without a significant drag penalty.

The final aircraft design was assessed against the requirement specification to identify its fulfilment of the criteria and overall success. While suitable for the scope of this project, a full audit report could be generated to validate the consistency of the design more rigorously against the specification.

8.7 Noise

The underwing engine position and the selection of chevron nozzles reduced the baseline aircraft's external noise levels, though the incorporation of high or ultra-high BPR and geared turbofan engines would have a drastic impact on noise reduction. However, this is beyond the scope of the project. Meanwhile, the acoustic liners are effective at cabin noise reduction, though have no impact on community noise levels. A more sophisticated cabin noise estimation method should be applied in the detailed design stage.

8.8 Emissions

Though some estimation of the aircraft's NO_x footprint was possible, more sophisticated calculations should be applied to find the emissions of both CO_2 and NO_x more accurately. The zero-emission variant cuts out all carbon emissions, though may increase NO_x emissions due to the higher combustion temperature of hydrogen. The scope of the project did not allow detailed consideration of tank insulation materials, so further analysis should be carried out. Even though the hydrogen combustion solution satisfies the specified emission levels, difficulties associated with the fuel storage, systems and airport infrastructure will likely increase DOCs.

9 Way of Working

9.1 Project management

From the beginning of the project, the importance of good teamwork has been emphasised. This began with activities to get to know the team and improve cohesion before the task was tackled. This helped the team understand the different ways of working and kickstarted good levels of communication that persisted through most of the project. While specialist roles were not initially laid out, they naturally fell into place quite quickly due to the range of interests each team member demonstrated.

A waterfall working methodology was established for a clear and structured approach to meet the final deadline within the tight time constraint. However, the importance of adaptability was emphasised due to the complex nature of the multi-disciplinary project, facilitating a more fluid approach to the problem without being held back by red tape. This was achieved through iterative design development stages, each with design freezes and reviews. A Gantt chart was also produced to structure and track the required progress, though without very specific details to allow for better adaptability.

A document and version control role was also established to protect important documents, such as the datasheet, and to allow easy sharing of information. This role proved vital to the project's organisation and efficiency and helped every member to make a meaningful contribution to the final design.

9.2 Document Control

Configuration Management (CM) is a proven tool in the aerospace industry that manages changes across the life cycle of a product [42]. For this project, CM philosophies were applied to the definition of criteria and tasks, the implementation of systems engineering approaches for document control and the construction of the planning structure to ensure its smooth running and the maintenance of momentum. To facilitate this, the AASI specialist was given responsibility for change management and configuration status accounting so that change processes could be monitored and controlled in a centralised manner.

Changes applied to the design and its supporting documentation were controlled through a master data sheet (Excel) and a document management package (Microsoft Teams). This allowed the maintenance of valid and present information ready for retrieval by each team member. Different document management packages such as Trello, GitHub and Sharepoint were also considered, however, the preliminary design stage was run on Microsoft Teams and it was deemed an unnecessary risk to require team members to familiarise themselves with a new system during the project.

Figure 27 demonstrates the change control procedure, with proposed changes being requested from the AASI specialist. A team-wide evaluation of the change's impacts followed and, if the change was approved, the GA and datasheet would be updated to for the next design iteration.

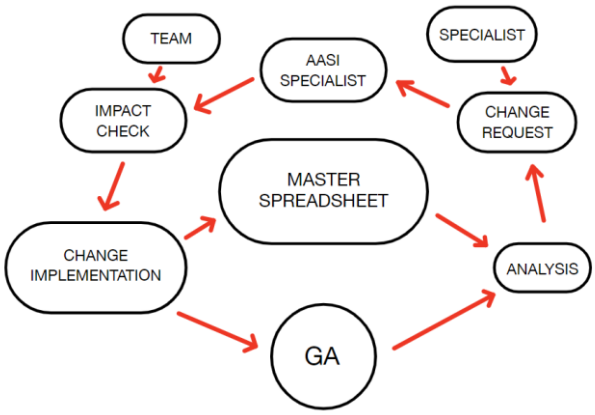

Figure 26: Version control methodology

10 Conclusions

The FW1 aircraft presents a novel design that fully satisfies the requirements laid out by Airbus in the 2020/2021 advanced student design project specification. The aircraft aims to meet the key design driver of minimum fuel burn over a 500nmi study mission, producing a block fuel 29% less than that of the A220-100. It has been demonstrated that, even with DOC savings relegated to a secondary driver position, the aircraft still exhibits improvements in this area, with a 9.8% saving over the same mission when compared to the A220-100. While fuel burn data is not provided for the 1000nmi design mission, it is reasonable to assume, based on the performance in fuel burn and DOCs of the study mission, that the aircraft will, at minimum, be in a competitive position financially for such a mission. The improved fuel burn also serves to reduce the risk of client profitability drops due to the volatility of fuel prices and the uncertain future of emission regulations.

An aircraft concept was also presented that satisfied the zero-emission requirement with relatively few design changes through modification of the existing engines to burn hydrogen fuel and an increase in fuselage length to facilitate fuel storage. However, a significant amount of further research, assessment and design would be required to fully realise this solution.

The multidisciplinary design approach has facilitated the design of a successful aircraft, despite limited opportunity for in-person meetings and teamwork. While there are areas that could benefit from further analysis and dedicated design, FW1 believes that the promise of the baseline aircraft is evident, and the concept should be taken into the detailed design phased for optimisation of the airframe at all levels. Furthermore, the zero-emission solution laid out satisfies the carbon emission requirements and could result in a successful aircraft after further work.

11 References

[1] Eurostat, “Air Transport Statistics,” December 2019. [Online]. Available: https://ec.europa.eu/eurostat/statistics-explained/index.php/Air_transport_statistics#Total_passenger_transport_to.2Ffrom_Intra-EU-28_represented_almost_half_of_the_total_air_passenger_transport. [Accessed 31 October 2020].

[2] Airbus, “Global Market Forecast,” 2019. [Online]. Available: https://www.airbus.com/aircraft/market/global-market-forecast.html. [Accessed 31 October 2020].

[3] Anon, “A220 Doc's & fuel burn v2,” 2020. [Online]. Available: https://www.ole.bris.ac.uk/webapps/blackboard/content/listContent.jsp?course_id=_241120_1&content_id=_4936289_1. [Accessed 15 12 2020].

[4] M. Niu, Airframe Structural Design, Hong Kong: Hong Kong Conmilit Press, 1999.

[5] EASA, “Easy Access Rules for Large aeroplanes,” 23 11 2018. [Online]. Available: https://www.easa.europa.eu/document-library/easy-access-rules/easy-access-rules-large-aeroplanes-cs-25. [Accessed 15 12 202].

[6] J. Roskam, Airplane Design, 1985.

[7] E. Torenbeek, Synthesis of Subsonic Airplane Design, Delft University Press, 1982.

[8] M. Sadraey, “Aerospace Series List Design and Analysis of Composite Structures: With applications to aerospace Structures,” in *Aircraft Design*, John Wiley & Sons, Ltd, 2013.

[9] D. Calderon, J. Cooper, M. Lowenberg, S. Neild and E. Coetzee, “Sizing High-Aspect-Ratio Wings with a Geometrically Nonlinear Beam Model,” *Journal of Aircraft*, vol. 56, no. 4, 2019.

[10] T. Engelbracht, “Aerodynamic and Stability & Control prediction in preliminary a/c design,” November 2009. [Online]. Available: https://www.ole.bris.ac.uk/bbcswebdav/pid-4936315-dt-content-rid-16854685_2/xid-16854685_2.

[11] G. L. Z. S. e. a. G. Qiao, “A review of electromechanical actuators for More/All electric aircraft systems,” *Proceedings of the Institution of Mechanical Engineers, Part C: Journal of Mechanical Engineering Science* , vol. 232, no. 22, pp. 4128-4151, 2018.

[12] P. Sforza, “Chapter 7 - Landing Gear Design,” in *Commercial Airplane Design Principles*, Butterworth-Heinemann, 2014, pp. 251-300.

[13] FAA, “COMFAA 3.0,” 14 8 2014. [Online]. Available: https://www.airporttech.tc.faa.gov/Products/Airport-Safety-Papers-Publications/Airport-Safety-Detail/ArtMID/3682/ArticleID/10/COMFAA-30. [Accessed 15 12 2020].

[14] Boeing, “Operational Advantages of Carbon Brakes,” 2009. [Online]. Available: https://www.boeing.com/commercial/aeromagazine/articles/qtr_03_09/article_05_1.html. [Accessed 15 12 2020].

[15] C. Brady, “Boeing 737 Landing Gear,” 1999. [Online]. Available: http://www.b737.org.uk/landinggear.htm. [Accessed 12 15 2020].

[16] D. Collin, “Overview of Aviation Noise Research Effort Supported by the European Union,” 2016. [Online]. Available: https://www.icao.int/environmental-

protection/Documents/EnvironmentalReports/2016/ENVReport2016_pg38-41.pdf. [Accessed 15 12 2020].

[17] R. Cabell, N. Schiller, J. Mabe, R. Ruggeri and G. Butler, "Feedback Control of a Morphing Chevron for Takeoff and Cruise Noise Reduction," in *ACTIVE*, Williamsburg, Virginia, 2004.

[18] A. Kempton, "Acoustic Liners for Modern Aero-Engines," 2011. [Online]. Available: https://www.win.tue.nl/ceas-asc/Workshop15/CEAS-ASC_XNoise-EV_K1_Kempton.pdf. [Accessed 17 12 2020].

[19] Anon, "Noise Control (Suppression)," Perdue School of Aeronautics and Astronautics, [Online]. Available: https://engineering.purdue.edu/~propulsi/propulsion/jets/basics/noise.html. [Accessed 17 12 2020].

[20] P. Ravetta, R. Burdisso, W. Ng, M. Khorrami and R. Stoker, "Screening of Potential Landing Gear Noise Control Devices at Virginia Tech for QTD II Flight Test," in *13th AIAA/CEAS Aeroacoustics Conference*, Rome, 2007.

[21] D. Giesecke, M. Lehmler, J. Friedrichs, J. Blinstrub, L. Bertsch and W. Heinze, "Evaluation of ultra-high bypass ratio engines for an over-wing aircraft configuration," *GPPS*, vol. 2, pp. 493-515, 2018.

[22] D. Lockney, "Aircraft Geared Architecture Reduces Fuel Cost and Noise," NASA Spinoff, 2015. [Online]. Available: https://spinoff.nasa.gov/Spinoff2015/t_1.html. [Accessed 17 12 2020].

[23] R. Shupe, K. Zaman and D. Papamoschou, "Effect of Wedge-Shaped Deflectors on Flow Fields of Dual-Stream Jets," in *13th AIAA/CEAS Aeroacoustics Conference*, Rome, 2007.

[24] Y. Guo, "On noise reduction by flap side-edge fences," *Journal of Sound and Vibration*, vol. 277, no. 1, pp. 369-390, 2004.

[25] F. Catalano, P. Vanuchi and L. Correa, "Wind Tunnel Testing of Porous Devices for the Reduction of Flap Side-Edge Noise," in *28th Congress of the International Council of the Aeronautical Sciences*, Brisbane, 2012.

[26] A. Finez, E. Jondeau, M. Roger and M. Jacob, "Broadband Noise Reduction with Trailing Edge Brushes," in *16th AIAA/CEAS Aeroacoustics Conference*, Stockholm, 2010.

[27] F. Hutcheson, T. Brooks and W. Humphreys, "Noise Radiation from a Continuous Mold-Line Link Flap Configuration," in *14th AIAA/CEAS Aeroacoustics Conference*, Vancouver, 2008.

[28] R. Erfani, H. Zare-Behtash, C. Hale and K. Kontis, "Development of DBD Plasma Actuators: The Double Encapsulated Electrode," *Acta Astronautica*, vol. 109, pp. 132-143, 2015.

[29] H. Siller, M. Jacob and U. Michel, "Flow and Noise Modification by Suction and Blowing on a Rod-Airfoil Configuration," in *11th AIAA/CEAS Aeroacoustics Conference*, Monterey, 2005.

[30] Aviation Benefits Beyond Borders, "Chevron Nozzles Reduce Noise," Air Transport Action Group, 27 6 2013. [Online]. Available: https://aviationbenefits.org/newswire/2013/06/chevron-nozzles-reduce-noise/#:~:text=As%20long%20ago%20as%202001,about%201%20dB(A). . [Accessed 15 12 2020].

[31] M. Dannemann, M. Kucher, E. Kunze, N. Modler, K. Knobloch, L. Enghardt, E. Sarradj and K. Hoschler, "Experimental Study of Advanced Helmholtz Resonator Liners with Increased Acoustic Performance by Utilising Material Damping Materials," *Applied Sciences*, vol. 8, no. 10, 15 10 2018.

[32] P. Ravetta, M. Khorrami, R. Burdisso and D. Wisda, “Acoustic Measurements of a Large Civil Transport Main Landing Gear Model,” in *22nd AIAA/CEAS Aeroacoustics Conference*, Lyon, France, 2016.

[33] A. Zaporozhets, V. Tokarev and K. Attenborough, Aircraft Noise: Assessment, Prediction and Control, Oxon: Spon Press, 2011.

[34] D. Heaton, “Simplified Noise Method, AVDASI 4 Resource List,” 2020. [Online]. Available: https://www.ole.bris.ac.uk/webapps/blackboard/content/listContent.jsp?course_id=_241120_1&content_id=_4936282_1&mode=reset. [Accessed 15 12 2020].

[35] EASA, “Emissions Databank,” 8 2020. [Online]. Available: https://www.easa.europa.eu/domains/environment/icao-aircraft-engine-emissions-databank. [Accessed 15 12 2020].

[36] ICAO, “ICAO Annex 16: Environmental Protection, Volume II -- Aircraft Engine Emissions,” 7 2008. [Online]. Available: https://law.resource.org/pub/us/cfr/ibr/004/icao.annex.16.v2.2008.pdf . [Accessed 15 12 2020].

[37] Roland Berger, “Hydrogen / A Future Fuel for Aviation?,” 03 2020. [Online]. Available: https://www.rolandberger.com/publications/publication_pdf/roland_berger_hydrogen_the_future_fuel_for_aviation.pdf. [Accessed 15 12 2020].

[38] D. Verstraete, “The Potential of Liquid Hydrogen for Long Range Aircraft Propulsion,” Cranfield University, Cranfield, 2009.

[39] C. Harley, “Aerodynamic Performance of Low Form Factor Spoilers,” University of Manchester, Manchester, 2010.

[40] D. P. Raymer, Aircraft Design: A Conceptual Approach, Second Edition, American Institute of Aeronautics and Astronautics, 1992.

[41] Anon, “AEA DOC Estimation Method,” 2013. [Online]. Available: https://www.ole.bris.ac.uk/bbcswebdav/pid-4936325-dt-content-rid-16854285_2/courses/AENGM0060_2020_TB-1/AENGM0060_2019_TB-1_ImportedContent_20190924095256/AEA-DOC-Calcs.pdf. [Accessed 31 October 2020].

[42] Y. Xu, M. Malisetty and M. Round, “Configuration Management in Aerospace Industry,” in *2nd International Through-Life Engineering Services Conference*, 2013.